

<https://doi.org/10.1038/s42003-024-06937-5>

The biogeography of the Amazonian tree flora



A list of authors and their affiliations appears at the end of the paper

We describe the geographical variation in tree species composition across Amazonian forests and show how environmental conditions are associated with species turnover. Our analyses are based on 2023 forest inventory plots (1 ha) that provide abundance data for a total of 5188 tree species. Within-plot species composition reflected both local environmental conditions (especially soil nutrients and hydrology) and geographical regions. A broader-scale view of species turnover was obtained by interpolating the relative tree species abundances over Amazonia into 47,441 0.1-degree grid cells. Two main dimensions of spatial change in tree species composition were identified. The first was a gradient between western Amazonia at the Andean forelands (with young geology and relatively nutrient-rich soils) and central–eastern Amazonia associated with the Guiana and Brazilian Shields (with more ancient geology and poor soils). The second gradient was between the wet forests of the northwest and the drier forests in southern Amazonia. Isolines linking cells of similar composition crossed major Amazonian rivers, suggesting that tree species distributions are not limited by rivers. Even though some areas of relatively sharp species turnover were identified, mostly the tree species composition changed gradually over large extents, which does not support delimiting clear discrete biogeographic regions within Amazonia.

Biogeography aims to describe, explain, and ultimately predict patterns of distribution and diversity at a variety of taxonomic levels¹. It has been a century-long quest to achieve these aims for the complex distributional patterns of biodiversity in Amazonia^{2,3}, an area formed by the tropical rain forests of the Amazon basin and Guiana shield. These forests are of global interest, as they arguably support the highest biodiversity on Earth^{4–8}. The total richness of the Amazonian tree flora has been estimated at ~16,000 species^{8,9}, with most species having geographically restricted ranges and small to very small population sizes. Furthermore, even the most abundant trees in Amazonia, despite being relatively more widespread, tend to dominate under specific environments⁸.

Existing biogeographical classifications of Amazonia have often defined centres of endemism coinciding with large interfluvial areas^{10–14}. This follows early models on the distribution patterns of vertebrate species that focused on the role of large rivers in separating species and triggering speciation – the riverine barrier hypothesis¹⁵. Although large rivers can act as effective barriers for land plants in some context¹⁶, studies on plant species have provided varying results^{17–20}, depending on the taxa under analysis, often resulting in weak or no support for large rivers as effective barriers for land plants. Another hypothesis proposed that the climatic oscillations during the Pleistocene both triggered speciation and affected species range dynamics in Amazonia – the Pleistocene refuge hypothesis²¹. According to

this hypothesis, tropical rain forest retraction–expansion dynamics was a key driver limiting species ranges during dry glacial periods and determining range expansions from the most consistently wet regions (i.e., refuges) during wetter interglacial periods. However, the high complexity of both the Amazonian forests themselves and the potential footprint of Pleistocene climatic oscillations on habitat availability for the numerous species that form the Amazon forests make it difficult to test the original refuge hypothesis, though it has stimulated a vigorous research agenda^{22,23}. The ecoregion approach, in turn, has used a combination of biological, ecological, and geographical proxies to derive a biogeographical classification²⁴. Other biogeographical classifications have been proposed based on the geographical distribution of soil classes²⁵, and understory floristic gradients as interpolated using remote sensing²⁶. Several recent studies have acknowledged the potential importance of edaphic and climatic factors, as well as of evolutionary and ecological processes at different temporal and spatial scales, on contemporary broad-scale distributional and diversity patterns of Amazonian trees and other plants^{8,20,23,26–31}. It has also been suggested that geographical barriers and climatic oscillations have had little effect on the distribution of land plants across Amazonia, but that geographical distance among populations can limit gene flow sufficiently to trigger speciation in geographically restricted areas – the dispersal assembly hypothesis³².

✉ e-mail: hans.terstegee@naturalis.nl

It remains a daunting task to draw biogeographical inferences from a relatively poorly explored region such as Amazonia, which has enormous shortfalls in biological knowledge^{28,33–38} and collecting density, i.e., data deficiencies and sampling bias^{33,35,39,40}. Despite the lack of data, much progress has been made in working with scarce spatial data by employing new analytical methods to circumvent problems of data scarcity for environmental characteristics and species occurrence (e.g., soil base cation concentration^{41,42} and beta diversity^{43,44}), and joining disparate efforts to advance our understanding on the distribution of tree species diversity, composition and abundance across Amazonia^{8,45–47}. Especially in the last decades of the 20th century, the number of forest inventories for Amazonian tropical rain forests has risen fast, allowing a more comprehensive view on tree diversity across Amazonia (e.g. ref. 45). However, quantitative tests of the biogeographical pattern of Amazonian tree communities are scarce and based on incomplete presence/absence data^{44,48} or on genus-level identifications and very coarse spatial resolution²⁹; but see Luize et al.⁴⁹, unveiling the role of dispersal and phylogenetic niche conservatism on phylogenetic compositional changes over Amazonia.

Here, making use of a set of 2,023 tree inventory plots with tree species abundance data, distributed well across Amazonia (Supplementary Fig. 1), we investigate how tree species composition varies across spatial and environmental gradients, with eyes on both ecological and biogeographical patterns. We start by ordering the tree species compositional dissimilarity between forest inventory plots, using Principal Coordinate Analysis (PCoA), to assess: (i) how the local variation on compositional turnover relates with the local variation in Amazonian forest types and among geographical regions within Amazonia; and (ii) how compositional turnover varies along spatial and environmental gradients representing edaphic and climatic features. We then use the observed abundances of tree species in each inventory plot to produce a broad-scale view of compositional turnover across Amazonia. After deriving grid layers, at the resolution of 0.1-degree grid cells (~121 km²), for the distribution of tree species' relative abundances

over the Amazon, we ordered, using Detrended Correspondence Analysis (DCA), the grid cell communities (i.e., species relative abundances over the grid cells). The resulting DCA scores are mapped over Amazonia to depict broad-scale tree species compositional turnover across the region. The maps of tree species compositional turnover were used to interpret the compositional turnover associations with geographic and broad-scale edaphic and climatic variation across the region and allowed the definition of floristic transitional zones – where changes of tree species turnover are sharper over short geographic distances. Finally, we estimated the tree species' niche position (optimum) and breadth (tolerance) for climatic, edaphic, and compositional dimensions to show how the compositional turnover patterns are determined by the ecological distribution of species over existing gradients.

Results

Plot-level patterns in tree species composition

The Principal Coordinates Analysis (PCoA) ordination shows that compositional turnover at the plot level is related to both broad ecological forest categories (Fig. 1a and Supplementary Fig. 2) and geographical location (Fig. 1b and Supplementary Fig. 3). Although there is substantial overlap among the geographical regions (Fig. 1b and Supplementary Fig. 3c), in general terms the first ordination axis (PCoA1) represents a gradient from southwestern Amazonia (with low scores) through central Amazonia to the Guiana Shield (with high scores; see also Supplementary Fig. 3). At the same time (Fig. 1a and Supplementary Fig. 2), the first ordination axis corresponds to a gradient in soil fertility (with poor soils having higher values than rich soils), and the second axis separates seasonally inundated (VA, IG) and permanently waterlogged (SW) forests (with high scores) from the non-inundated forests (TFGS, TFBS, TFPB, PZ, with lower scores). Linear regressions confirmed these observations, with the main floristic gradient (PCoA1) strongly related to sum of base cations in the soil ($R^2_{adj} = 0.27$, $P = 0.01$, Supplementary Fig. 4a), and the second floristic gradient (PCoA2)

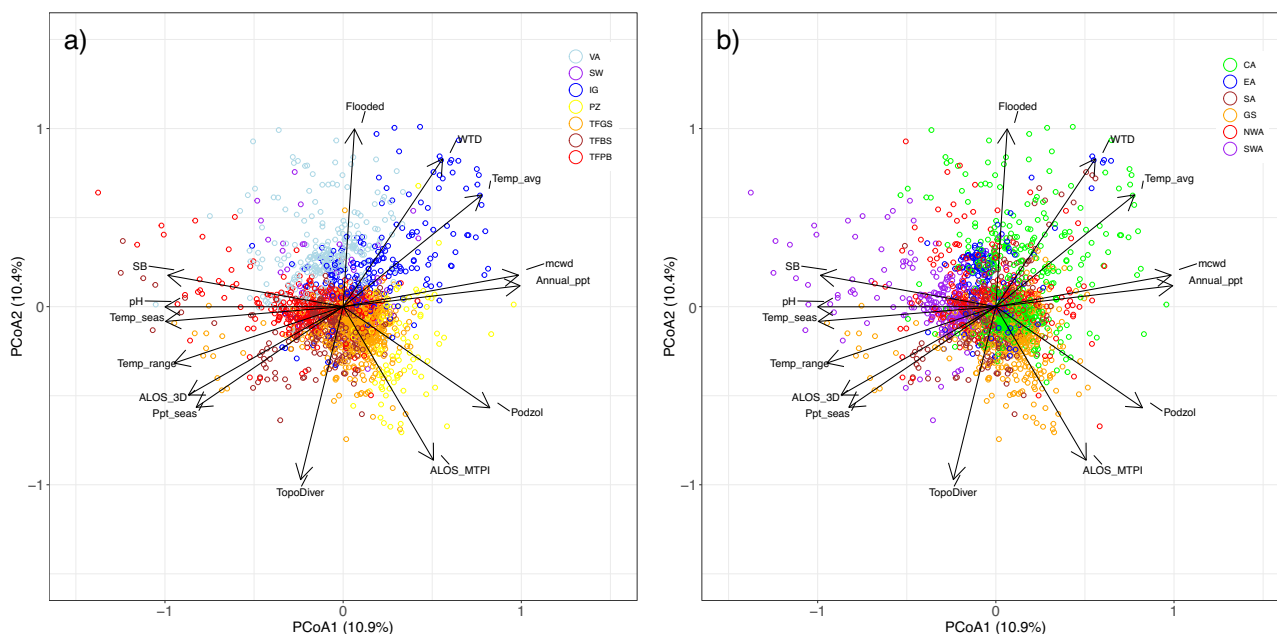


Fig. 1 | Variation in composition and relative abundance of 5188 tree species in 2023 forest-inventory plots (1 ha) across Amazonian forests. Ordination biplots showing the two first principal components with inventory plots coloured by (a) ecological forest categories based on hydrology and soil characteristics and (b) geographical regions. **a** Ecological categories: VA, Várzea forests; SW, swamp forests; IG, igapó forests; PZ, white-sand (podzol) forests; TFGS, terra-firme on the Guiana Shield; TFBS terra-firme on the Brazilian Shield, TFPB terra-firme on the Pebas sedimentary basin. **b** Geographical regions: CA Central Amazonia, EA Eastern Amazonia, SA Southern Amazonia, GS Guiana Shield, NWA Northwestern Amazonia, SWA Southwestern Amazonia. Arrows indicate vectors constructed with *envfit*(⁸¹) for 14 environmental predictors: Flooded flooding vs. non-flooding terrains, WTD water table depth, Temp_avg average annual temperature, MCWD maximum climatological water deficit), Annal_ppt Annual Rainfall, Podzol White Sand vs. Clay-Silt terrains, ALOS_MTPi Multiscale Topographic Position Index, TopoDiver Topographic Diversity Index, Ppt_sea precipitation seasonality, ALOS_3D elevation, Temp_range temperature range, Temp_seas temperature seasonality, pH soil pH, SB soil sum of bases.

Amazonia, SWA Southwestern Amazonia. Arrows indicate vectors constructed with *envfit*(⁸¹) for 14 environmental predictors: Flooded flooding vs. non-flooding terrains, WTD water table depth, Temp_avg average annual temperature, MCWD maximum climatological water deficit), Annal_ppt Annual Rainfall, Podzol White Sand vs. Clay-Silt terrains, ALOS_MTPi Multiscale Topographic Position Index, TopoDiver Topographic Diversity Index, Ppt_sea precipitation seasonality, ALOS_3D elevation, Temp_range temperature range, Temp_seas temperature seasonality, pH soil pH, SB soil sum of bases.

Table 1 | The association of environmental conditions and the variation in the tree species composition of Amazonian forests

Rank	Environmental predictor	R ²	AdjR ² _{Cum}	F	AIC
<i>RDA Model 1: [PCoA axis 1] ~ 14 environmental predictors</i>					
1	Soil base cation concentration (SB)	0.27	0.27	764.6	-6438.3
2	Temperature seasonality	0.09	0.36	280.2	-6699.1
3	Podzol	0.04	0.4	122.7	-6816.5
4	Elevation (ALOS_3D)	0.03	0.42	86	-6898.9
5	Maximum climatological water deficit (MCWD)	0.01	0.44	47.4	-6943.8
6	Soil pH	0.01	0.45	44.1	-6985.6
7	Precipitation seasonality	0.01	0.45	26.2	-7009.7
8	Total annual rainfall	0	0.46	13.2	-7020.9
9	Mean annual temperature	0	0.46	13.3	-7032.3
10	Flooded	0	0.46	13.1	-7043.3
11	Topographic diversity (TopoDiver)	0	0.47	8.1	-7049.4
12	Groundwater table depth (WTD)	0	0.47	3.7	-7051.1
13	Multi-scale topographic index (MTPI)	0	0.47	5.8	-7054.9
14	Temperature range	Forward selection procedure stopped (not selected)			
<i>RDA Model 2: [PCoA axis 2] ~ 14 environmental predictors</i>					
1	Flooded	0.42	0.42	1450.4	-6988.9
2	Podzol	0.01	0.43	39.9	-7026.5
3	Topographic diversity (TopoDiver)	0.01	0.44	44	-7068.1
4	Precipitation seasonality	0.01	0.45	40.8	-7106.6
5	Soil base cation concentration (SB)	0.01	0.46	21.4	-7126
6	Mean annual temperature	0.01	0.46	26.9	-7150.8
7	Temperature range	0	0.47	14.9	-7163.7
8	Elevation (ALOS_3D)	0	0.47	25.9	-7187.5
9	Maximum climatological water deficit (MCWD)	0	0.48	7.3	-7192.9
10 to 14	Multi-scale topographic index (MTPI), soil pH, temperature seasonality, total annual rainfall, groundwater table depth (WTD)	Forward selection procedure stopped (not selected)			
<i>RDA Model 3: [PCoA axis 1: PCoA axis 2] ~ 14 environmental predictors</i>					
1	Flooded	0.21	0.21	470.9	-4694.5
2	Soil base cation concentration (SB)	0.18	0.39	520.2	-5149.5
3	Maximum climatological water deficit (MCWD)	0.04	0.43	132.5	-5275.6
4	Podzol	0.03	0.46	88.4	-5360.1
5	Soil pH	0.02	0.48	69.8	-5426.8
6	Precipitation seasonality	0.01	0.48	17.5	-5442.3
7	Temperature range	0.01	0.49	17.9	-5458.2
8	Mean annual temperature	0.00	0.49	14.9	-5471.1
9	Topographic diversity (TopoDiver)	0.00	0.49	10.1	-5479.3
10	Elevation (ALOS_3D)	0.00	0.50	13.4	-5490.7
11 to 14	Total annual rainfall, temperature seasonality, multi-scale topographic	Forward selection procedure stopped (not selected)			

Table 1 (continued) | The association of environmental conditions and the variation in the tree species composition of Amazonian forests

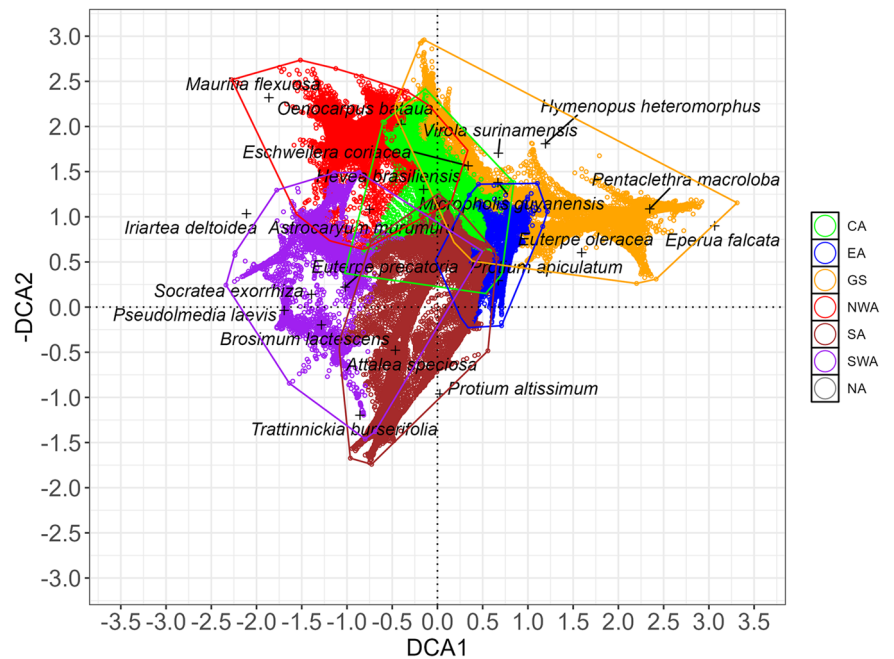
Rank	Environmental predictor	R ²	AdjR ² _{Cum}	F	AIC
index (MTPI), groundwater table depth (WTD)					
<i>RDA Model 4: residuals[RDA model: [PCoA axis 1:PCoA axis 2] ~ 93 MEMs] ~ 14 environmental predictors</i>					
1	Flooded	0.094	0.09	209.4	-6171.3
2	Soil base cation concentration (SB)	0.047	0.14	110.8	-6277.4
3	Podzol	0.016	0.16	39.3	-6314.4
4	Temperature range	0.005	0.16	13.2	-6325.6
5	Elevation (ALOS_3D)	0.002	0.16	3.1	-6326.7
6	Mean annual temperature	0.001	0.16	3.8	-6328.5
7 to 14	Temperature seasonality, total annual rainfall, precipitation seasonality, maximum climatological water deficit (MCWD), topographic diversity (TopoDiver), multi-scale topographic index (MTPI), soil pH, groundwater table depth (WTD)	Forward selection procedure stopped (not selected)			

The results of RDA models relating PCoA scores and 14 environmental predictors. The first model adjusts only the PCoA axis 1, the second model adjusts only the PCoA axis 2, the third model adjusts both PCoA axis at once, and the fourth model uses the residuals of the RDA model relating the PCoA scores and the spatial predictors (93 selected Moran's Eigenvector Maps MEMs) to adjust the 14 environmental predictors. PCoA axes scores were obtained from the pair-wise Bray-Curtis dissimilarities among 2,023 forest-inventory plots. Predictors are ordered from lowest to highest AIC. The R² and F statistics were estimated using permutation tests under a forward selection procedure.

strongly related to whether the plot was inundated or not ($R^2_{adj} = 0.42$, $P = 0.01$). Forward selection identified 13 environmental predictors significantly related to PCoA1, and together these explained 47% of the variation in tree species abundances along PCoA1 (Table 1). In addition to the importance of soil sum of bases, temperature seasonality ($R^2_{adj} = 0.09$, $P = 0.01$) and white sand soils ($R^2_{adj} = 0.04$, $P = 0.01$) were significant environmental predictors for the first ordination axis (Table 1). For the second floristic gradient (PCoA2), nine environmental predictors were selected, which together explained 43% of the variation in tree species abundances along PCoA2 (Table 1). In this case, flooding was clearly the most important and the other eight predictors added little explanatory power (Table 1). Although there is a lot of overlap, the ordination at plot level supports a general pattern of turnover in tree species composition between forests in ecological regimes (Fig. 1), traditionally recognised as distinct forest types, such as terra-firme, white-sand, and seasonally flooded forests, which can be geographically proximate over a landscape.

Besides the significant influence of environmental gradients to the variation in each PCoA axis separately (Table 1), and in both axes together (RDA model: [PCoA axis 1: PCoA axis 2] ~ 14 Environmental predictors, $R^2_{adj} = 0.47$; $P = 0.001$), we also found spatially structured variation on the compositional turnover measured at plot-level (RDA model: [PCoA axis 1: PCoA axis 2] ~ 93 MEMs, $R^2_{adj} = 0.51$, $P = 0.001$). After partitioning out the relative effect of environmental and spatial predictors on tree species composition, there is a significant spatial structure in the environmental predictors, shown as the shared influence of environmental and spatial predictors on tree species composition (joint Environmental + Spatial fraction of variation partition, $R^2_{adj} = 0.33$, $P = 0.001$). Ruling out this joint environmental + spatial effect, the environmental predictors alone add a little less variation on tree species composition (unique environmental fraction of variation partition, $R^2_{adj} = 0.14$; $P = 0.001$) than the spatial predictors (MEMs) alone (unique spatial fraction of variation partition,

Fig. 2 | Variation in interpolated composition and relative abundance of 5,188 tree species in 47,441 grid cells (0.1-degree squares) across Amazonian forests. Ordination biplots showing the two first DCA axes with grid cells coloured by geographic region: CA Central Amazonia, EA Eastern Amazonia, GS Guiana Shield, NWA Northwestern Amazonia, SWA Southwestern Amazonia, SA Southern Amazonia. Black marks show the average position for the abundance distribution of the 20 tree species with the highest interpolated total abundance. The distributions of these species in geographical and ordination space are shown in Supplementary Figs. 5–24.



$R^2_{\text{adj}} = 0.18$; $P = 0.0001$). The first two environmental predictors, explaining most of the variation in both PCoA axes (Flooded and Soil base cation concentration (SB) Table 1, RDA Model 3), are the same predictors responsible for most of the non-spatially structured compositional variation (i.e., the residuals of the spatial RDA model (PCoA [1:2] ~ 93 MEMs), Table 1 RDA Model 4). Although, some of the environmental predictors, explaining most of PCoA axes variation (maximum climatological water deficit (MCWD), Soil pH, Table 1 RDA Model 3), actually explain a small and non-significant amount of the non-spatially structured compositional variation ($R^2 \leq 0.001$, $P > 0.05$, Table 1 RDA Model 4).

Patterns in grid-level tree species composition and turnover

When the effect of local environmental variation was averaged out by interpolating relative species abundances at the resolution of 0.1° grid cells (Fig. 2), the main axis of variation in tree species composition (DCA1) clearly showed a longitudinal gradient from western Amazonian forests (SWA and NWA) through central and southern Amazonia (CA and SA) towards Eastern Amazonia (EA) and the Guiana shield (GS). Along the second axis (DCA2), the strongest contrast was between the southern regions (SA and SWA, with low scores) and northern and central regions (NWA, CA, and parts of GS, with high scores), with EA being intermediate and showing much less variation than the other regions. In fact, the biplot in Fig. 2 clearly reflects the geographical outlay of the Amazonian forest.

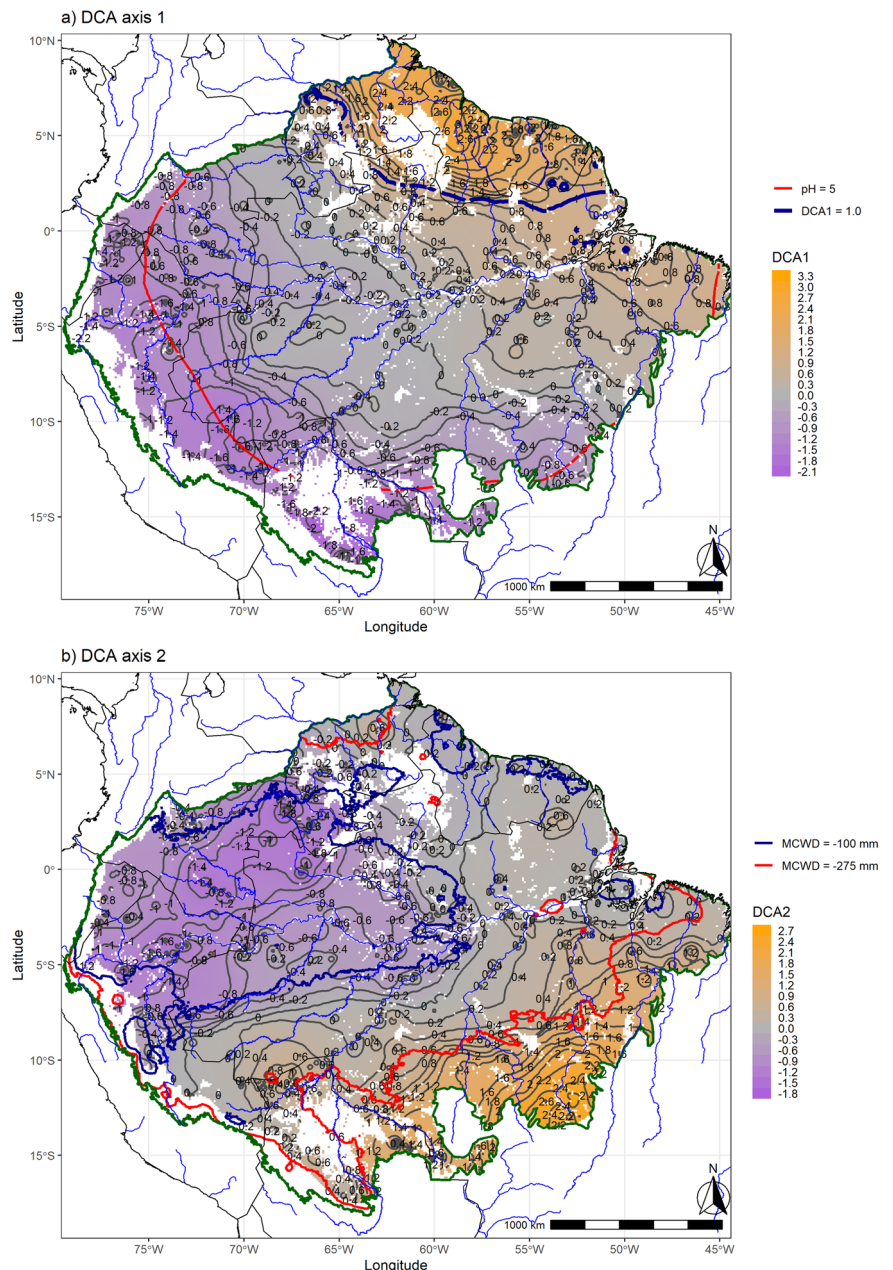
The general impression from the grid-level DCA ordination is that floristic transitions across Amazonia are rather gradual among the geographical regions, as adjacent regions have relatively similar floristic composition. This was confirmed when the DCA scores were plotted on the actual map of Amazonia (Fig. 3): tree species composition changed gradually over large geographical distances. The gradual change in composition recovered by DCA1 ran from the Andean forelands to the Guiana Shield (Fig. 3a). Over most of Amazonia, isolines of the DCA1 scores were far apart, indicating gradual species turnover across space, but some zones showed sharper turnover. These zones of intense compositional turnover over short geographical distances were concordant with the confluence of tree species' geographical and environmental range limits, even for very common tree species (e.g., *Eperua falcata*, *E. coriacea* and *Trattinnickia burserifolia*, Supplementary Figs. 5–24). These areas of sharper tree species turnover were also in agreement with abrupt changes in climatological and edaphic attributes (Fig. 3a). In particular, DCA1 showed two zones of sharp turnover. The first zone ran in the east-west direction largely coincident with the

headwaters of the rivers draining from the Guiana highlands and Acarai mountains (see the isoline of DCA1 value 1 in Fig. 3a), separating the Guianas from the rest of Amazonia. The second zone of relatively sharp turnover ran across Amazonian lowlands in the west in a north-south orientation coinciding with changes in average soil acidity (pH) and soil base cation concentration (SB), which are higher on the western than the eastern side of the transition zone (Fig. 3a). The gradual changes in tree species composition indicated by DCA2 ran from north-western Amazonia to south-eastern Amazonia (Fig. 3b). In DCA2, the zone of sharpest turnover ran in the east-west direction, being even more steep in the southern part of the Amazon basin (Fig. 3b, isoline of MCWD value -275). A slightly more gradual turnover zone can be seen further north running right across several major tributaries of the Amazon River (e.g., Juruá, Purus, Madeira), and also crossing the Amazon River itself. The zones of sharp turnover shown by DCA2 largely follow a divide between wetter and dryer climates. The wetter areas encompass the upper Negro River, the Japurá/Caquetá, the Içá/Putumayo, and the Napo River basins, and the dryer areas the headwaters of the Tapajós and Xingú Rivers (Fig. 3b).

Species distributions along environmental and compositional gradients

The most common Amazonian tree species are widespread across Amazonia but show diverging centres of distribution along the compositional gradient recovered by the grid-level DCA ordination (Supplementary Figs. 5–24), suggesting they occupy different niche positions. Indeed, the niche positions of individual species are well distributed along both the climatic gradients (annual rainfall, maximum climatological water deficit), and the edaphic gradients (soil sum of bases, pH) (Fig. 4a–d), and also along the compositional gradients (based on DCA scores of the grid cells) (Fig. 4e, f). Furthermore, as suggested by the species niche breadths, most species tend to occupy only a relatively small part of the observed gradient, while a few species show broad niche breadths (Fig. 4). Among the 20 most common tree species in our plot dataset (based on the sum of plot-level abundances), those with the strongest preference for very wet climates (highest niche positions (WA) for annual rainfall, Fig. 4a) were *Rinorea riana*, *Oenocarpus bacaba*, and *Rinorea racemosa*. Fifty-three species exclusively occurred in plots with maximum climatological water deficit equal to zero (Fig. 4b); *Eperua falcata*, *Oenocarpus bataua*, and *Mauritia flexuosa* were the three species among the most common ones with niche position for MCWD close to zero (i.e., wettest places in Fig. 4b), in contrast

Fig. 3 | Maps of the broad-scale spatial variation of tree species composition across Amazonia. Scores of (a) DCA Axis 1, (b) DCA Axis 2 (both from Fig. 2). In both maps, grey lines are the isolines linking equal levels of DCA scores, with the spatial distance between consecutive isolines being inversely related to the rate of compositional change across space and used to mark sharp compositional turnover zones (if closer together) or smoother compositional turnover (consecutive isolines further apart). In (a), the blue isoline corresponds to DCA score of 1.0 and the red isoline to soil pH = 5 (west of that line having a soil pH >5). In (b), the red isoline corresponds to maximum climatological water deficit (MCWD) = -275 mm (south of that line having MCWD < -275), and the blue isoline to MCWD = -100 (west that line having MCWD > -100). The dark green line delimits the Amazonian tropical forests⁹⁵, with white areas within these limits corresponding to montane areas (above 500 m elevation) and non-forested habitats such as savannas. Major river courses are shown in blue. Base map source for countries: <https://www.naturalearthdata.com/>; rivers⁶¹. Maps created with custom R⁸⁸ script.



to *Protium altissimum* that is among the most common species with low niche position values for MCWD (i.e., drier end of the gradient in Fig. 4b). All 20 most common species were distributed in the middle of the gradient in soil fertility (i.e. show niche position for the logarithm of soil sum of bases within -0.5 and 0.5, Fig. 4c), and in the acidic part of the soil pH gradient (i.e. have niche position for soil pH between 4.2 and 5.5). Two of the 20 most common species (*Eperua falcata*, and *Pentaclethra macroloba*) had a niche position value for DCA1 > 1 (Fig. 4d), corresponding to main occurrence area in the Guiana Shield (Fig. 2). Very common species occurring mainly in western Amazonia (DCA1 < -0.8) were *Pseudolmedia laevis* and *Iriartea deltoidea*, and these were largely the same species as the ones with sum of bases optimum > -0.06. Common species from the drier areas in southern Amazonia (DCA2 > 0.4) included *Theobroma speciosum*, *Amaioua guianensis*, *Amphiodon effusus*, *Metrodorea flavida*, and *Protium heptaphyllum*. The niche positions (niche optima) and niche breadths (tolerances) for all 5,188 tree species are given in Supplementary table 1.

The associations of species niche positions on compositional and environmental gradients show that species placed at both ends of the

compositional gradient are also placed at the ends of the environmental gradients (Fig. 5), supporting that species niche segregation does influence compositional turnover. Edaphic gradients (pH, SB) segregate the species along the first compositional dimension (DCA1; Fig. 5a, b), while the species composition along the second compositional dimension (DCA2) is segregated along the water availability gradient (Annual rainfall, MCWD; Fig. 5c, d). Species occupying the upper ends of the main compositional gradient tend to occupy a smaller fraction of the existing gradient.

Discussion

In Amazonia, tree-inventory plots generally do not share a large number of tree species⁵⁰. The high compositional differentiation between forest plots (even in the same area) reflects sampling by 1-ha plots: all species that actually exist at a site cannot be sampled with the limited number of stems that fit within 1-ha plot⁵¹. Nevertheless, our analyses recovered compositional gradients that are related to environmental factors, even after removing spatially structured environmental variation. The first PCoA axis (corresponding to the strongest gradient in tree species composition at the

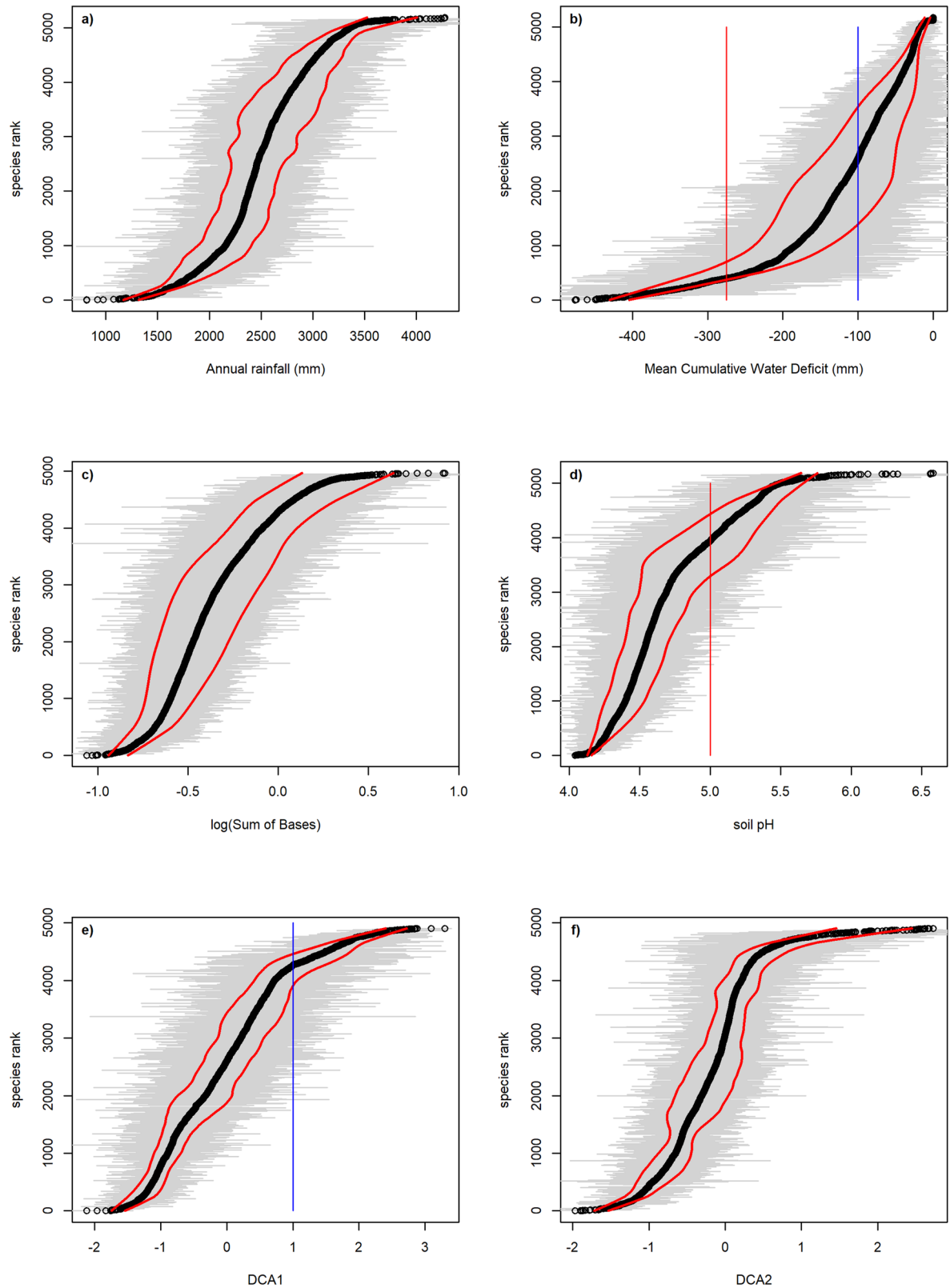


Fig. 4 | Niche positions and niche breadths of 5188 tree species along environmental and compositional gradients in Amazonia as calculated with data from 2023 1-ha forest-inventory plots. Gradients along the x axis: (a) Annual rainfall (mm); (b) maximum climatological water deficit (mm); (c) log(soil sum of bases (Ca +Mg+K)); (d) soil acidity (pH); (e) DCA1 scores from Fig. 2; and (f) DCA2 scores from Fig. 2. The black dots mark the mean niche position or optimum (weighted average value) for each species and the grey lines depict the niche breadths or

tolerance (\pm standard deviation for the variable in sites where the species was observed). The red lines show the mean niche breadth (determined by loess regression). Coloured lines correspond to the lines also visible in Fig. 3 (DCA1, DCA2, pH, MCWD). Species are shown from bottom to top in the order of increasing niche position. (See supplementary data 1 for the niche breadth and position values of all tree species).

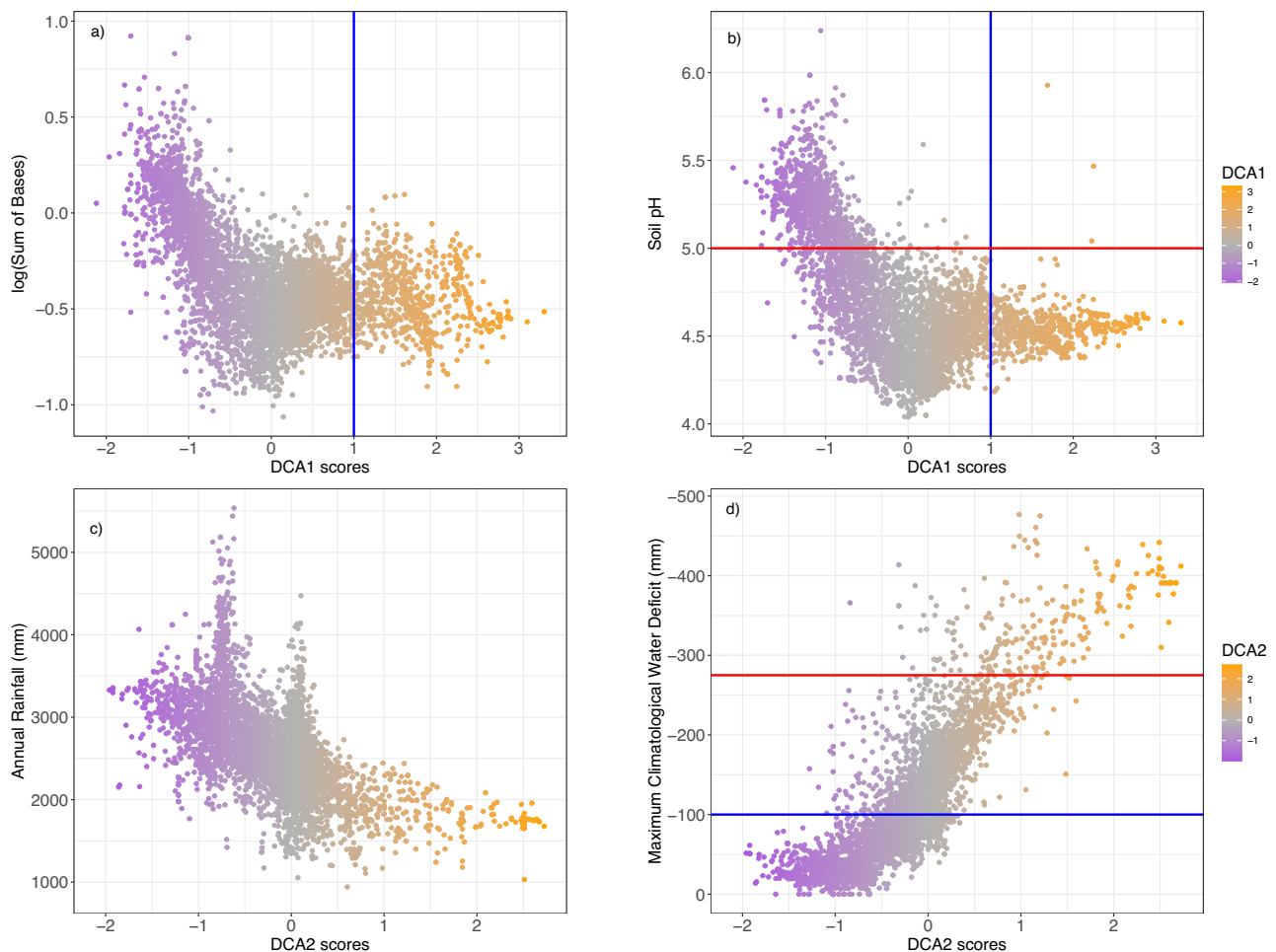


Fig. 5 | The associations of species niche positions on compositional and environmental gradients. In the first row the species niche positions on the DCA1 scores gradient in relation to edaphic niche position gradients: (a) Soil sum of bases, (b) Soil pH. The second row shows the species niche positions along the DCA2 scores

gradient in relation to climatic gradients: (c) Annual Rainfall, (d) Maximum climatological water deficit. Plot colours correspond to colours in Fig. 3. Coloured lines correspond to the lines (DCA1, pH, MCWD) also visible in Fig. 3.

plot level) reflects mainly differences in mean soil fertility, which also shows a geographical east-to-west gradient. This is congruent with several recent studies that have emphasised the role of soil nutrient status as a driver of floristic patterns^{20,26,29–31,48,52,53}. The second PCoA axis relates to hydrology (whether or not the terrain was seasonally flooded or permanently water-logged) and characteristics of the flooding waters (white vs. black water). This conforms with the traditional classification of Amazonian forests, corresponding to use of the names of forest types in this paper.

Changing the spatial unit of analysis from the plot level to the grid cell level removed the influence of local ecological conditions. At the same time, it also reduced the importance of uncertainties related to local compositional affinities and the distribution of species across environmental and geographical gradients. For instance, whereas the average 1-ha forest-inventory plot contained only 94 tree species (1.8% of the known tree species pool in Amazonia), the interpolation predicted an average of 1,474 species (29% of the species pool⁵⁴) for the 0.1-degree grid cells, which is comparable with the range of 800–900 tree species found in large (25 ha) forest inventory plots⁵⁵. Furthermore, given that in Amazonia most tree species are rare^{8,9} and that rare species are more likely to provide information on how areas differ in composition, the use of interpolated population sizes of species brought the advantage keeping the species rarity structure in the data. When the local-scale ecological variation was eliminated by spatially interpolating species abundances and aggregating them into 0.1-degree grid cells, the continuous and gradual change in tree species composition became even more evident, conforming to a view already suggested long ago²

By projecting the DCA scores over the map of Amazonia, we identified some areas of sharp compositional change over relatively short geographical distances. The overall broad-scale compositional patterns were still related to patterns in soil fertility and climate (Figs. 4 and 5), which is consistent with the proposal that environmental variation drives much of the biogeographical differentiation across Amazonian forest assemblages^{26,30,48}. Our results support earlier research that showed gradual changes in the generic composition of trees across Amazonia²⁹ but have much higher spatial resolution (0.1° rather than 4 by 6-degree grid cell), as well taxonomic precision (species rather than genera), and in terms of environmental data quality.

Our results support a gradual east to west change in tree species composition across Amazonia, in agreement with previous studies^{29,47,56}. The strong associations of tree species composition with soil base cation concentrations (SB), flooding condition, seasonality in temperature and precipitation, podzolization, and topography suggest those environmental gradients as important environmental constraints of tree species distribution across Amazonia, in agreement with earlier regional studies^{30,31,47,57}. In western Amazonian forests, for instance, the narrow tolerance of species for seasonal droughts is the main environmental factor limiting species distribution⁵⁸. However, we found tree species composition overlapping among regions (Figs. 1 and 2), suggesting that trees are not impaired by geographical delimitations within Amazonia (see, for example, Supplementary Figs. 5–24) and/or that several tree species tolerate a broad range of environmental conditions (Fig. 4). It is expected that tree species with

relatively narrow niches, as well as those with narrow geographical ranges, will be the ones with distribution restricted to one part of the existing environmental gradient within the large geographical extent, covered by tropical rain forests of Amazonia.

Based on the spatial distribution of the DCA scores, we identified four zones of relatively sharp spatial turnover in tree species composition (i.e., floristic transitional zones) within Amazonia. Importantly, each of those floristic transitional zones was associated with major changes along distinct environmental gradients. For example, the floristic transitional zone in the Northeastern part of Amazonia is coincident with the interfluvial divide between the Amazon Basin and the river basins draining from the highlands of the Guiana Shield and Acarai Mountains. The forests along this floristic transitional zone were more dynamic in terms of vegetational changes induced by climatic variations over the last 30,000 years^{59,60}, and are still characterised by a dry transverse belt from the Rio Branco, Rupununi and Sipaliwini savannas to the Trombetas-Tapajós confluence with the Amazon River. This may be the most important biogeographical divide in Amazonia, that is less marked, however, in the lowlands of the northern coastal river basins⁶¹ (i.e., French Guiana and the Amapá State in Brazil). The other three floristic transitional areas, however, do not show clear biogeographical barriers controlling the compositional changes over short distances. Rather, continuous changes in environment along the lowlands are likely influencing compositional turnover here. The floristic transitional zone of western part of Amazonia can be associated with changes in soil fertility (SB) and acidity (pH) and perhaps species with Andean affinity. Forests found west of that transitional area (i.e., closer to the Andean foothills) grow on relatively younger sediments that form fertile and more basic soils⁴². This compositional transition zone is largely coincident with a previously reported compositional turnover zone of biogeographical importance^{20,26} that crosses both the middle-upper Juruá river and the main Amazon River. A third floristic transitional zone forms a belt traversing the major white-water tributaries of the Amazon River (i.e., Juruá, Purus and Madeira rivers) and the Amazon River itself (Fig. 3b – blue isoline). This floristic transitional zone delimitates the region with lower elevation across Amazonia; it separates the forests at the southern and northern borders of the Amazon basin from the forests close to the Amazon River main stem. The region that this fourth floristic transitional zone crosses the Amazon river provide support for earlier biogeographic delimitations of várzea forests in the Amazon river floodplains⁶². The southern floristic transitional zone is largely coincident with changes from a wetter to relatively drier climate, relatively close to transition zone between the tropical rain forest and savanna biomes.

Further studies could consider the temporal dynamics of these environmental gradients to shed light on the dynamic feature of those floristic transitional zones. Historical floristic dynamics among surrounding biomes and even within the open to dense lowland rain forests may have influenced the formation of zones of sharp floristic turnover. For example, floristic legacies from Andean-centred tree species, whose distribution is skewed to mild temperatures of higher montane forests in the tropical Andes^{5,63} were reported in earlier studies in the Amazon lowland rain forests^{33,64} and are included in the western floristic zone we identified (e.g., *Ilex*, *Panopsis*). Similar reasoning may apply to the area of floristic transition in the southern part of Amazonia, which is relatively close to the confluence between the tree species in seasonally deciduous forests within the Cerrado biome and the tree species occurring in the wetter forests of the Amazonian lowlands and has been rather dynamic over historical times⁶⁵. The sharp compositional changes between the tropical rain forests of the Guiana Shield and the Amazon basin were perhaps earlier based on geographic and ecologic barriers (e.g., mountains, dry areas), which were more pronounced in the past, but nowadays they are likely to be maintained by ecological sorting along relatively sharp environmental gradients and limited dispersal.

The pattern of floristic compositional changes across Amazonian forests, at both resolutions we evaluated, is consistent with the description of a longitudinal gradient in floristic composition across Amazonia, with the forests in the Western Amazonia gradually differing from the forests on the Guiana Shield^{29,66}. Despite the overriding effect of local environmental

conditions at the plot level, the east-west compositional changes across Amazonia were apparent even in the plot data (Fig. 1). This is most likely controlled by the general east-west gradient in local environmental conditions, and perhaps by species dispersal across Amazonia.

Changes in tree species composition among local assemblages are primarily related to differences in soil fertility and to flooding conditions. Changes in tree species composition across Amazonian forests are mostly gradual over large geographical extents, but more sharply over relatively short geographical distances in certain areas. Zones of pronounced tree species turnover over short geographical distances tend to show abrupt changes in broad-scale gradients of soil fertility, temperature seasonality, and the seasonal availability or deficit of water. The Amazonian tree flora is assembled by several thousand tree species partitioned over the environmental gradients; the floristic transitional zones in Amazonia are not concordant with putative biogeographical barriers hampering the definition of strictly defined biogeographical units based on the Amazonian tree flora.

Methods

Forest inventory database and environmental correlates

Our tree-inventory data (March 2024 - ATDN20240303) are part of the Amazon Tree Diversity Network^{8,9,45}, which contained 2023 tree-inventory plots (Supplementary Fig. 1) with information on species composition and abundance. Most of tree-inventories were for 1-ha size and sampled trees with a diameter at breast height (DBH, at 1.30 m) or above tabular roots ≥ 10 cm (for plot metadata, see Supplementary table 2). Species synonymy was updated following ref. 54, but harmonizing names with the World Flora Online⁶⁷. Species with a *confer* (*cf.*) identification were accepted as belonging to the named species, while those with *affinis* (*aff.*) were accepted only at the genus level and therefore removed from this analysis. The final community matrix comprised 2,023 plots and 5,188 accepted tree species.

The plot coordinates were used to classify each plot into one of six geographic regions (Supplementary Fig. 1): (i) Northwestern Amazonia (NWA), (ii) Southwestern Amazonia (SWA), (iii) Central Amazonia (CA), (iv) Southern Amazonia (SA), (v) Eastern Amazonia (EA) and (vi) Guiana Shield (GS). Plot metadata were used to classify the forests into seven ecological categories (Supplementary Fig. 1). Four of these refer to non-inundated areas (terra-firme): (i) Terra-firme over the sedimentary basin (TFPB), (ii) Terra-Firme over the Brazilian Shield formation (TFBS), (iii) Terra-Firme over the Guiana Shield formation (TFGS), and (iv) Terra-Firme over podzols (i.e., White-Sand Forests (PZ)). The other three refer to wetland forests: (i) Várzea (VA; seasonally inundated by a white-water rivers), (ii) Igapó (IG; seasonally inundated by a black or clear-water rivers), and (iii) Swamp (SW; permanently poorly drained).

To evaluate the association of tree species composition with environmental conditions, a total of 12 continuous environmental attributes were extracted from gridded data. A soil acidity (pH) surface for entire Amazonia was created with a loess model (with a span of 0.2, a degree of 2, using Gaussian fitting) based on measurements of soil pH from soil profiles available from several sources^{41,42,68–72} (Supplementary Fig. 25). As a measure of nutrient availability, we used the logarithm of soil base cation concentration (SB; Ca+Mg+K), as provided by Zuquim et al.⁴². Climatic data was obtained from CHELSA⁷³. We used three variables for temperature (mean annual temperature, temperature range, and temperature seasonality) and two for precipitation (total annual rainfall, precipitation seasonality). We also estimated the maximum climatological water deficit (MCWD), which can be considered a measure of seasonal drought. This was calculated as the cumulative rainfall deficit of consecutive months with ≤ 100 mm of precipitation from 1981–2020 as measured by CHIRPS^{74–76}. The water-table depth was extracted from a gridded layer produced by Fan et al.⁷⁷. Three topographic variables (elevation, multi-scale topographic index, topographic diversity index) were obtained from the digital surface models of the ALOS World 3D^{78,79}. In addition to the 12 continuous environmental predictors, we included two categorical environmental predictors that discriminate the major forest types of Amazonia. For that we classified the sites into Flooded vs. Non-flooded (i.e., Seasonally flooded

forests vs. Upland non-flooded forests), and Podzol vs. Non-Podzol (i.e., White sand forests vs. Forests on silt and clay soils). Environmental attributes were selected beforehand to represent edaphic and climatic features with recognised importance for tree species distribution. Also, before proceeding with the analysis, we tested the variance inflation factor (VIF)⁸⁰ of the 14 environmental predictors to assure that there are not multicollinearity issues between predictors. Highest VIF was obtained for elevation (VIF = 7.4), but still lower than the threshold of VIF = 10 indicating a strong collinearity between predictors⁸⁰. We then followed the analysis using all the 14 environmental predictors.

Analysis of plot-level data

We first explored gradients in tree species composition at the plot level, i.e., using the original tree inventory data. We calculated floristic dissimilarities between the plots using the Bray-Curtis index based on relative abundance data. As some pairs of plots were completely dissimilar to each other, we used the extended dissimilarities to replace the dissimilarity values saturated to the maximum value of unity (c.a. 9% of the total pairwise dissimilarities) with a path across single stepping-stone points⁸¹, providing ecologically-realistic dissimilarities between plots that share no species⁸². The resulting dissimilarity matrix was analysed using Principal Coordinates Analysis (PCoA), and scatterplots for the scores of the first two axes were used to visually interpret the variation in tree species composition in relation to geographical location and ecological classes of Amazonian forests. We focused our interpretation on the first two PCoA axes, together capturing 21.3% of variation in the dissimilarity matrix, as subsequent axes do not capture more than 6% of total variation. To aid on the interpretation of the variation in tree species composition in relation with the environmental gradients, we added, to the PCoA scatterplot, vectors showing the direction towards greatest environmental changes and increase of association with the ordination configuration. We, then, quantified the strengths (adjusted R^2) of the linear relationships between PCoA scores and the 14 available environmental predictors using Redundancy Analysis (RDA) with forward selection to evaluate which are the environmental gradients explaining most of variation in tree species composition. The forward selection fits a linear model of each predictor at a time and tests their adjusted R^2 against randomly permuted fitting.

Given the geographic extent covered by the inventory-plots included in the ATDN database, and the inherent spatially irregular sampling design of the inventory-plots, it is expected that the spatial structure of plots (e.g., geographic clusters) exerts an influence both on the measured environmental gradients and on the tree species compositional turnover^{49,83,84}. To evaluate the relative influence of unique spatial fraction, unique environmental fraction, and their shared effect (environmental + spatial) on tree species composition, we applied a variation partitioning approach, using the set of 14 environmental predictors plus a selected set of Moran's eigenvector maps (MEMs) as spatial predictors. To select the spatial weighting matrix (SWM) used to derive the MEMs, we used three graph-based criteria of connectivity (Gabriel's graph, Relative neighbourhood graph, Minimum spanning tree) and weighting following a linear decreasing function of plot coordinates distances, as recommended in ref. 85. The double diagonalization of the of the SWM results in a large set of MEMs, which were further selected based on the optimisation of adjusted R^2 using forward selection with a double-stopping criterion, following⁸⁶. To test the significance of the unique spatial fraction and the shared environmental + spatial fraction of the variation partition model, we used Moran spectral randomisations, which are spatially constrained permutations that provide robust estimates of the significance of model adjustments^{83,84,87}. Finally, we quantified, using RDA with forward selection, the adjusted R^2 of each environmental predictor fitting only the unique environmental fraction (i.e., the residuals of the model relating both PCoA axes and the MEMs spatial predictors) to access the influence of non-spatially structured environmental gradients on tree species compositional turnover.

All analyses were done in the R environment⁸⁸. Extended dissimilarities were computed with the 'stepacross' function, environmental vectors were

fitted with the 'envfit' function, and variation partitioning were performed with the 'varpart' function of the "Vegan" library⁸¹. PCoA were computed with the 'pco' function of the "labdsv" library⁸⁹. The optimisation of selected SWM and the selection of subset of MEMs were performed with the 'listw.select' function, the spatially constrained permutation tests of the unique and the shared fractions of variation partitioning were performed with the 'msr' and 'envspace.test' functions, and the RDA with forward selection with the 'forward.sel' function of the "adespatial" library⁹⁰.

Analysis of grid-level data

Plot-level analyses are strongly affected by local ecological effects, which can vary considerably over short geographical distances (e.g., plots representing inundated vs. non-inundated forests can be in close proximity to each other). To remove this effect and focus on more broad-scale biogeographical patterns, we divided Amazonia into 47,441 grid cells at the resolution of 0.1 arc degrees (~121 km²) and estimated the relative abundance of each tree species for each grid cell using the spatial interpolation method of ter Steege et al.^{8,91}. As a relative abundance measure, we used $RA_i = n_i / N_p$, where n_i equals the number of stems of species i and N_p the total number of stems in the plot (including unidentified trees). For all 5188 species with a valid name in the plots, we constructed an inverse distance weighting (IDW) model for RA_i , with a distance-decay power of 2, a maximum number of plots used for each local estimation of 150, and a maximum distance parameter of 4 degrees.

We performed a Detrended Correspondence Analysis (DCA) on the grid-level community matrix to map the broad-scale variation of tree species composition across Amazonia. This is for two reasons, we assumed that there are no strict biogeographical boundaries in Amazonia, and DCA is a perfect way of describing gradients (see below); PCoA is based on similarities among plots (in this case cells) and would average out the gradients too much. DCA is based on weighted averaging and to balance the influence of common species in the ordination pattern, we used DCA without down-weighting rare species, which are most of the species in Amazonia^{8,9}. The response curve of species is assumed to be unimodal, with the average being the mean niche position and the standard deviation being a measure of niche breadth⁹². The results were visualised both with traditional ordination scatterplots and by plotting the DCA axis scores on a map of Amazonia. In the DCA ordination plot, we also visualised the distributions of the 20 most abundant tree species (those with the largest sum of relative abundances over all grid cells). On the map of Amazonia, we added isolines that link similar levels of DCA scores to assess species turnover rates: when consecutive DCA isolines are relatively close to each other, species turnover across space is sharper than when consecutive DCA isolines are relatively far from each other. To highlight the association between areas of sharper species turnover and existing environmental gradients, we overlaid the isolines for soil pH over the map of the first DCA axis and the isolines for maximum climatological water deficit with the map of the second DCA axis. To define the level for the environmental gradient isolines to be overlaid over the DCA maps, we evaluated the point of inflection in the curve associating the species distributional ranges along the environmental scales. DCA was performed using the function 'decorana' of the "Vegan" R library⁸¹, with standard settings and without down-weighting rare species.

Gradients and species niche breadth

To aid in the interpretation of the broad-scale variation of tree species composition across Amazonia, we computed the species' mean niche positions and breadths along environmental and compositional gradients. The mean niche position was computed by calculating weighted averages (WA)⁹³ of the plot-wise species relative abundances for four environmental variables (annual rainfall, maximum cumulative water deficit, sum of bases, pH) and for the compositional gradients obtained from the grid-level DCA analyses (DCA axes 1 and 2 scores). The values of each independent variable were extracted from the corresponding raster data using the coordinates of the forest inventory plots. Weighted Averaging scores (mean niche position or optimum) for those variables were calculated for each species using the

'wascores' function of the "Vegan" library⁸¹. We used ± 1 standard deviation as a measure of the species niche breadth.

Statistics and reproducibility

All tests were carried out with all plots ($n = 2023$).

Reporting summary

Further information on research design is available in the Nature Portfolio Reporting Summary linked to this article.

Data availability

All plot metadata is included in supplementary table 2. The code to reproduce analysis and figures, the PCoA scores by plot, the grided community matrix and the mean niche position (weighted averages) and niche breadth for the species, are publicly available through FigShare⁹⁴. Additional plot-based data is available upon reasonable request by contacting the corresponding author.

Code availability

All custom R code used in the analysis and visualisation of the data is publicly available through FigShare⁹⁴. This code can be used to produce all figures and Supplementary figures.

Received: 18 April 2024; Accepted: 23 September 2024;

Published online: 02 October 2024

References

- Lomolino, M. V., Riddle, B. R. & Whittaker, R. J. *Biogeography* (Fifth edition). (Oxford University Press, 2017).
- Ducke, A. & Black, G. A. Phytogeographical notes on the Brazilian Amazon. *Acad. Bras. Cienc.* **25**, 1–46 (1953).
- Huber, J. Novitates florae amazonicae. *Bol. do Mus. Goeldi de Historia Nat. e Ethnographia* **6**, 60–90 (1909).
- Antonelli, A. et al. Amazonia is the primary source of Neotropical biodiversity. *Proc. Natl Acad. Sci. USA* <https://doi.org/10.1073/pnas.1713819115> (2018).
- Antonelli, A. & Sanmartin, I. Why are there so many plant species in the Neotropics? *TAXON* **60**, 403–414 (2011).
- Cupertino-Eisenlohr, M. A., Oliveira-Filho, A. T. & Simon, M. F. Patterns of variation in tree composition and richness in Neotropical Non-Flooded Evergreen Forests. *Appl. Veg. Sci.* **24**, e12522 (2021).
- Raven, P. H. et al. The distribution of biodiversity richness in the tropics. *Sci. Adv.* **6**, eabc6228 (2020).
- ter Steege, H. et al. Hyperdominance in the Amazonian tree flora. *Science* **342**, 1243092 (2013).
- ter Steege, H. et al. Biased-corrected richness estimates for the Amazonian tree flora. *Sci. Rep.* **10**, 10130 (2020).
- Oliveira, U., Vasconcelos, M. F. & Santos, A. J. Biogeography of Amazon birds: rivers limit species composition, but not areas of endemism. *Sci. Rep.* **7**, 2992 (2017).
- Pirani, R. M. et al. Testing main Amazonian rivers as barriers across time and space within widespread taxa. *J. Biogeogr.* **46**, 2444–2456 (2019).
- Ribas, C. C. & Aleixo, A. Diversity and evolution of Amazonian birds: implications for conservation and biogeography. *Acad. Bras. Cienc.* **91**, e20190218 (2019).
- Ribas, C. C., Aleixo, A., Nogueira, A. C. R., Miyaki, C. Y. & Cracraft, J. A palaeobiogeographic model for biotic diversification within Amazonia over the past three million years. *Proc. R. Soc. B Biol. Sci.* **279**, 681–689 (2012).
- Silva, S. M. et al. A dynamic continental moisture gradient drove Amazonian bird diversification. *Sci. Adv.* **5**, eaat5752 (2019).
- Wallace, A. R. On the monkeys of the Amazon. *Ann. Mag. Nat. Hist.* **14**, 451–454 (1854).
- Melo Santos, A. M., Cavalcanti, D. R., Silva, J. M. C., & Tabarelli, M. Biogeographical relationships among tropical forests in north-eastern Brazil. *J. Biogeogr.* **34**, 437–446 (2007).
- Honorio Coronado, E. N., Dexter, K. G., Hart, M. L., Phillips, O. L. & Pennington, R. T. Comparative phylogeography of five widespread tree species: Insights into the history of western Amazonia. *Ecol. Evol.* **9**, 7333–7345 (2019).
- Nazareno, A. G., Dick, C. W. & Lohmann, L. G. Wide but not impermeable: Testing the riverine barrier hypothesis for an Amazonian plant species. *Mol. Ecol.* **26**, 3636–3648 (2017).
- Nazareno, A. G., Dick, C. W. & Lohmann, L. G. A biogeographic barrier test reveals a strong genetic structure for a canopy-emergent Amazon tree species. *Sci. Rep.* **9**, 18602 (2019).
- Tuomisto, H. et al. A compositional turnover zone of biogeographical magnitude within lowland Amazonia. *J. Biogeogr.* **43**, 2400–2411 (2016).
- Haffer, J. Speciation in Amazonian forest birds. *Science* **165**, 131–137 (1969).
- Baker, P. A. et al. *Neotropical Diversification: Patterns and Processes* (eds V. Rull & A. C. Carnaval) 51–70 (Springer International Publishing, 2020).
- Hooen, C. et al. Amazonia through time: andean uplift, climate change, landscape evolution, and biodiversity. *Science* **330**, 927–931 (2010).
- Olson, D. M. et al. Terrestrial Ecoregions of the World: A New Map of Life on Earth: a new global map of terrestrial ecoregions provides an innovative tool for conserving biodiversity. *BioScience* **51**, 933–938 (2001).
- Quesada, C. A. et al. Soils of Amazonia with particular reference to the RAINFOR sites. *Biogeosciences* **8**, 1415–1440 (2011).
- Tuomisto, H. et al. Discovering floristic and geocological gradients across Amazonia. *J. Biogeogr.* **46**, 1734–1748 (2019).
- Hooen, C. & Wesselingh, F. *Amazonia: Landscape And Species Evolution: A Look Into The Past* (John Wiley & Sons, 2011).
- Malhado, A. C. M. et al. The ecological biogeography of Amazonia. *Front. Biogeogr.* **5**, 103–112 (2012).
- ter Steege, H. et al. Continental-scale patterns of canopy tree composition and function across Amazonia. *Nature* **443**, 444–447 (2006).
- Tuomisto, H., Ruokolainen, K. & Yli-Halla, M. Dispersal, environment, and floristic variation of western Amazonian forests. *Science* **299**, 241–244 (2003).
- Higgins, M. A. et al. Geological control of floristic composition in Amazonian forests. *J. Biogeogr.* **38**, 2136–2149 (2011).
- Dexter, K. G. et al. Dispersal assembly of rain forest tree communities across the Amazon basin. *Proc. Natl Acad. Sci. USA* **114**, 2645–2650 (2017).
- Carvalho, R. L. et al. Pervasive gaps in Amazonian ecological research. *Curr. Biol.* **33**, 1–9 (2023).
- Feeley, K. Are we filling the data void? An assessment of the amount and extent of plant collection records and census data available for Tropical South America. *PLoS ONE* **10**, e0125629 (2015).
- Hopkins, M. J. G. Modelling the known and unknown plant biodiversity of the Amazon Basin. *J. Biogeogr.* **34**, 1400–1411 (2007).
- Hortal, J. et al. Seven shortfalls that beset large-scale knowledge of biodiversity. *Annu. Rev. Ecol. Evol. Syst.* **46**, 523–549 (2015).
- Milliken, W., Zappi, D., Sasaki, D., Hopkins, M. & Pennington, R. T. Amazon vegetation: how much don't we know and how much does it matter? *Kew Bull.* **65**, 691–709 (2010).
- Oliveira, U. et al. The strong influence of collection bias on biodiversity knowledge shortfalls of Brazilian terrestrial biodiversity. *Divers. Distrib.* **22**, 1232–1244 (2016).
- Antonelli, A. et al. Conceptual and empirical advances in Neotropical biodiversity research. *PeerJ* **6**, e5644 (2018).
- ter Steege, H. et al. The discovery of the Amazonian tree flora with an updated checklist of all known tree taxa. *Sci. Rep.* **6**, 29549 (2016).

41. Zuquim, G. et al. Making the most of scarce data: mapping soil gradients in data-poor areas using species occurrence records. *Methods Ecol. Evol.* **10**, 788–801 (2019).
42. Zuquim, G. et al. Introducing a map of soil base cation concentration, an ecologically relevant GIS-layer for Amazonian forests. *Geoderma Reg.* **33**, e00645 (2023).
43. Emilio, T. et al. Assessing the relationship between forest types and canopy tree beta diversity in Amazonia. *Ecography* **33**, 738–747 (2010).
44. Silva-Souza, K. J. P. & Souza, A. F. Woody plant subregions of the Amazon forest. *J. Ecol.* **108**, 2321–2335 (2020).
45. ter Steege, H. et al. Mapping density, diversity and species-richness of the Amazon tree flora. *Commun. Biol.* **6**, 1130 (2023).
46. ter Steege, H. et al. A spatial model of tree α -diversity and tree density for the Amazon. *Biodivers. Conserv.* **12**, 2255–2277 (2003).
47. Marca-Zevallos, M. J. et al. Local hydrological conditions influence tree diversity and composition across the Amazon basin. *Ecography* **2022**, e06125 (2022).
48. Oliveira-Filho, A. T. et al. On the floristic identity of Amazonian vegetation types. *Biotropica* **53**, 767–777 (2021).
49. Luize, B. G. et al. Geography and ecology shape the phylogenetic composition of Amazonian tree communities. *J. Biogeogr.* **51**, 1163–1184 (2024).
50. Bohlman, S. A. et al. Importance of soils, topography and geographic distance in structuring central Amazonian tree communities. *J. Veg. Sci.* **19**, 863–874 (2008).
51. Tuomisto, H. & Ruokolainen, K. Comment on “Disentangling the Drivers of β Diversity Along Latitudinal and Elevational Gradients”. *Science* **335**, 1573–1573 (2012).
52. Phillips, O. L. et al. Habitat association among Amazonian tree species: a landscape-scale approach. *J. Ecol.* **91**, 757–775 (2003).
53. Baldeck, C. A., Tupayachi, R., Sinca, F., Jaramillo, N. & Asner, G. P. Environmental drivers of tree community turnover in western Amazonian forests. *Ecography* **39**, 1089–1099 (2016).
54. ter Steege, H. et al. Towards a dynamic list of Amazonian tree species. *Sci. Rep.* **9**, 3501 (2019).
55. Duque, A. et al. Insights into regional patterns of Amazonian forest structure, diversity, and dominance from three large terra-firme forest dynamics plots. *Biodivers. Conserv.* **26**, 669–686 (2017).
56. Oliveira, A. A. & Nelson, B. W. Floristic relationships of terra firme forests in the Brazilian Amazon. *For. Ecol. Manag.* **146**, 169–179 (2001).
57. Duivenvoorden, J. F., Svenning, J.-C. & Wright, S. J. Beta diversity in tropical forests. *Science* **295**, 636–637 (2002).
58. Muelbert, A. E. et al. Seasonal drought limits tree species across the Neotropics. *Ecography* **40**, 618–629 (2016).
59. Costa, G. C. et al. Biome stability in South America over the last 30 kyr: Inferences from long-term vegetation dynamics and habitat modelling. *Glob. Ecol. Biogeogr.* **27**, 285–297 (2018).
60. van der Hammen, T. & Absy, M. L. Amazonia during the last glacial. *Palaeogeogr. Palaeoclimatol. Palaeoecol.* **109**, 247–261 (1994).
61. Venticinque, E. et al. An explicit GIS-based river basin framework for aquatic ecosystem conservation in the Amazon. *Earth Syst. Sci. Data* **8**, 651–661 (2016).
62. Albermaz, A. L. et al. Tree species compositional change and conservation implications in the white-water flooded forests of the Brazilian Amazon. *J. Biogeogr.* **39**, 869–883 (2012).
63. Gentry, A. H. Neotropical floristic diversity: phytogeographical connections between Central and South America, pleistocene climatic fluctuations, or an accident of the andean orogeny? *Ann. Mo. Bot. Gard.* **69**, 557–593 (1982).
64. Householder, J. E., Wittmann, F., Tobler, M. W. & Janovec, J. P. Montane bias in lowland Amazonian peatlands: plant assembly on heterogeneous landscapes and potential significance to palynological inference. *Palaeogeogr. Palaeoclimatol., Palaeoecol.* **423**, 138–148 (2015).
65. Mayle, F. E., Burbridge, R. & Killeen, T. J. Millennial-scale dynamics of Southern Amazonian Rain Forests. *Science* **290**, 2291–2294 (2000).
66. ter Steege, H. et al. Mapping density, diversity and species-richness of the Amazonian tree flora. *Commun. Biol.* **6**, 1130 (2023).
67. WFO (World Flora Online, 2024).
68. Batjes, N. H. Harmonized soil property values for broad-scale modelling (WISE30sec) with estimates of global soil carbon stocks. *Geoderma* **269**, 61–68 (2016).
69. Dijkshoorn, J. A., Huting, J. R. M. & Tempel, P. *Update of the 1:5 million Soil and Terrain Database for Latin America and the Caribbean (SOTERLAC; version 2.0)*. (ISRIC - World Soil Information, 2005).
70. Poels, R. L. H. *Soils Water And Nutrients In A Forest Ecosystem in Surinam*. PhD thesis (Wageningen University, 1987).
71. Quesada, C. A. et al. Variations in chemical and physical properties of Amazon forest soils in relation to their genesis. *Biogeosciences* **7**, 1515–1541 (2010).
72. van Kekem, A. J., Pulles, J. H. M. & Khan, Z. *Soils of the Rainforest in Central Guyana*. Vol. 2 (Tropenbos Guyana Programme, 1996).
73. Karger, D. N. et al. Climatologies at high resolution for the earth’s land surface areas. *Sci. Data* **4**, 170122 (2017).
74. Funk, C. et al. The climate hazards infrared precipitation with stations — a new environmental record for monitoring extremes. *Sci. Data* **2**, 150066 (2015).
75. Hirota, M., Holmgren, M., Van Nes, E. H. & Scheffer, M. Global resilience of tropical forest and Savanna to critical transitions. *Science* **334**, 232–235 (2011).
76. Malhado, A. C. M., Costa, M. H., de Lima, F. Z., Portilho, K. C. & Figueiredo, D. N. Seasonal leaf dynamics in an Amazonian tropical forest. *For. Ecol. Manag.* **258**, 1161–1165 (2009).
77. Fan, Y. & Li, H. Global patterns of groundwater table depth. *Science* **339**, 910 940–943 (2013).
78. Takaku, J., Tadono, T., Tsutsui, K. & Ichikawa, M. Validation of “AW3D” global dsm generated from alos prism. *ISPRS Ann. Photogramm. Remote Sens. Spat. Inf. Sci.* **III-4**, 25–31 (2016).
79. Theobald, D. M., Harrison-Atlas, D., Monahan, W. B. & Albano, C. M. Ecologically-relevant maps of landforms and physiographic diversity for climate adaptation planning. *PLoS ONE* **10**, e0143619 (2015).
80. Naimi, B., Hamm, N. A. S., Groen, T. A., Skidmore, A. K. & Toxopeus, A. G. Where is positional uncertainty a problem for species distribution modelling? *Ecography* **37**, 191–203 (2014).
81. The vegan Package. <http://vegan.r-forge.r-project.org/> (CRAN network, 2008).
82. De’ath, G. Extended dissimilarity: a method of robust estimation of ecological distances from high beta diversity data. *Plant Ecol.* **144**, 191–199 (1999).
83. Bauman, D., Vleminckx, J., Hardy, O. J. & Drouet, T. Testing and interpreting the shared space-environment fraction in variation partitioning analyses of ecological data. *Oikos* **128**, 274–285 (2019).
84. Clappe, S., Dray, S. & Peres-Neto, P. R. Beyond neutrality: disentangling the effects of species sorting and spurious correlations in community analysis. *Ecology* **99**, 1737–1747 (2018).
85. Bauman, D., Drouet, T., Fortin, M.-J. & Dray, S. Optimizing the choice of a spatial weighting matrix in eigenvector-based methods. *Ecology* **99**, 2159–2166 (2018).
86. Bauman, D., Drouet, T., Dray, S. & Vleminckx, J. Disentangling good from bad practices in the selection of spatial or phylogenetic eigenvectors. *Ecography* **41**, 1638–1649 (2018).
87. Wagner, H. H. & Dray, S. Generating spatially constrained null models for irregularly spaced data using Moran spectral randomization methods. *Methods Ecol. Evol.* **6**, 1169–1178 (2015).

88. R. Development Core Team. *R: A Language And Environment For Statistical Computing. Report No. ISBN 3-900051-07-0* (R Foundation for Statistical Computing, 2019).
89. Roberts, D. W. *Ordination and Multivariate Analysis for Ecology* (<https://cran.r-project.org/web/packages/labdsv/index.html>) (2023).
90. Dray, S. et al. *adespatial: Multivariate Multiscale Spatial Analysis* (<https://CRAN.R-project.org/package=adespatial>) (2021).
91. ter Steege, H. et al. Estimating the global conservation status of over 15,000 Amazonian tree species. *Sci. Adv.* **1**, e1500936 (2015).
92. Jongman, R. H. G., ter Braak, C. J. F. & van Tongeren, O. F. R. *Data Analysis In Community And Landscape Ecology*. 299 (Pudoc, 1987).
93. Whittaker, R. H. *Ordination of Plant Communities* (ed Robert H. Whittaker) 7-50 (Springer Netherlands, 1978).
94. Luize, B. G. & ter Steege, H. Analyses in “The Biogeography of the Amazonian Tree Flora”. *Figshare* <https://doi.org/10.6084/m9.figshare.26792731> (2024).
95. RAISG (<https://www.amazoniasocioambiental.org/en/>) (2020).

Acknowledgements

This paper is the result of the work of hundreds of different scientists and research institutions in the Amazon over the past 80 years. Without their hard work this analysis would have been impossible. We thank Charles Zartman for the use of plots from Jutai. BGL (<https://orcid.org/0000-0002-8384-8386>) acknowledge grants #2015/24554-0, #2019/24823-2, #2020/03379-4, and #2021/11670-3, #2021/10639-5 São Paulo Research Foundation (FAPESP). Ht.S., V.F.G. and R.S. were supported by grant 407232/2013-3 - PVE - MEC/MCTI/CAPES/CNPq/FAPs; P.I.P. had support for this work from CNPq (productivity grant 310885/2017-5) and FAPESP (research grant #09/53413-5); C.B. was supported by grant FAPESP 95/3058-0 - CRS 068/96 WWF Brasil - The Body Shop; D.S., J.F.M., J.E., P.P. and J.C. benefited from an “Investissement d’Avenir” grant managed by the Agence Nationale de la Recherche (CEBA: ANR-10-LABX-25-01); HLQ/MAP/JLLM received financial supported by MCT/CNPq/CT-INFRA/GEOMA #550373/2010-1 and # 457515/2012-0, and JLLM were supported by grant CAPES/PDSE # 88881.135761/2016-01 and CAPES/Fapespa #1530801; The Brazilian National Research Council (CNPq) provided a productivity grant to EMV (Grant 308040/2017-1); Floristic identification in plots in the RAINFOR forest monitoring network has been supported by the Natural Environment Research Council (grants NE/B503384/1, NE/ D01025X/1, NE/I02982X/1, NE/F005806/1, NE/ D005590/1 and NE/I028122/1) and the Gordon and Betty Moore Foundation; BMF is funded by FAPESP grant 2016/25086-3. BSM, BHMJ and OLP were supported by grants CNPq/CAPES/FAPS/BC-Newton Fund #441244/2016-5 and FAPEMAT/0589267/2016; T.W.H. was funded by National Science Foundation grant DEB-1556338; H.T. acknowledges grant DNR179. W.E.M.: plots in the PPBio system were financed by the INCT for Amazonian Biodiversity (CENBAM); the Program for Biodiversity Research in Western Amazonia (PPBio-AmOc) and a Productivity Grant (PQ - 301873/2016-0). Finally, we thank four reviewers for their questions and comments, which have greatly improved the manuscript.

Author contributions

Ht.S., B.G.L. and R.E. conceived the study; B.G.L., H.T., R.E., K.G.D., I.L.D.A., L.D.S.C., F.D.D.A.M., D.D.A.L.F., R.P.S., F.W., C.V.C., M.D.J.V.C., J.E.G., O.L.P., W.E.M., D.S., J.D.C.R., J.M., M.V.I., M.P.M., J.R.D.S.G., J.F.R., O.S.B., M.T.F.P., D.C.L., N.C.P., L.O.D., J.S., E.M.M.D.L.N., P.N.V., T.S.F.S., E.M.V., A.G.M., N.F.C.R., J.T., K.R.C., E.N.H.C., A.M.M., J.C.M., F.R.C., T.R.F., A.C.Q., N.C.A., C.E.Z., T.J.K., B.S.M., B.H.M., R.V., B.M., R.L.A., C.B., D.D.D.A., J.E., P.P., H.C., M.B.D.M., M.F.S., An.A., J.L.C., W.F.L., S.G.L., L.M.R., J.S., T.R.S., G.B.M., E.D.S.F., M.A.L., J.L.L.M., H.E.M.N., H.L.D.Q., C.C.V., G.A.A.C., R.B., P.R.S., A.I.A., B.B.L.C., T.R.B., Y.O.F., H.F.M., J.F.D., C.A.P., M.R.S., L.V.F., J.R.L., J.A.C., J.J.D.T., G.D., N.D., F.C.D., R.G., A.L., A.V., F.C.V., A.I.A.I., L.A., F.D., V.H.G., E.M.J., D.N., M.C.P.M., J.C.N., D.P.P.D.A., F.R.B., Y.K.B., R.D.S.C., F.A.C., F.C.D.S.,

K.J.F., R.G., T.H., J.E.H., M.P.P., J.J.P.I., M.R.P., D.D.J.R., J.B., E.B., I.B.D.S., M.J.F., J.F., P.V.F., M.C.G., C.L., J.C.L., B.E.V.Z., V.A.V., C.C., F.M.D., É.F., T.W.H., J.E.H., I.H., M.S., J.S., R.T., D.D., W.M., G.P.M., T.P., I.C.G.V., B.W.A., W.C., A.F., B.K., J.L.M.P., J.S.T., C.V., J.C., A.D.F., R.R.H., L.D.O.P., J.F.P., G.R., T.R.V.A., P.V.H., W.B., E.M.B., L.C.D.M.B., H.P.D.D., R.Z.G., T.G., G.P.G.G., B.H., A.B.J., Y.M., I.P.D.A.M., L.F.M.P., A.P., A.R., A.R.R., N.S., C.I.V., S.Z., E.L.Z., M.J.E., A.C., Y.A.C.M., D.F.C., J.B.P.C., B.M.F., D.G., M.H., M.K., G.L., L.T.M., M.T.N., A.A.O., M.M.P., H.R., M.R., V.V.S., M.N.U., G.V.D.H., E.V.T., T.M.V., M.A.A.R., C.B., H.B., S.C., L.F.C., W.F., C.F., R.L., C.M., I.M., G.A.P., A.T., L.E.U.G., D.V., R.Z., M.N.A., E.A.D.O., R.P.F., K.G.C., L.H., W.P.C., S.P., D.P., F.R.A., A.F.S., E.H.V.S., L.V.G., M.H., C.P. and Ht.S. conducted fieldwork and collected data with additional information; Ht.S., B.G.L. and H.T. analysed the data; B.G.L. and Ht.S. led the writing of the manuscript with assistance from K.G.D., H.T. and C.P.; B.G.L., H.T., R.E., K.G.D., I.L.D.A., L.D.S.C., F.D.D.A.M., D.D.A.L.F., R.P.S., F.W., C.V.C., M.D.J.V.C., J.E.G., O.L.P., W.E.M., D.S., J.D.C.R., J.M., M.V.I., M.P.M., J.R.D.S.G., J.F.R., O.S.B., M.T.F.P., D.C.L., N.C.P., L.O.D., J.S., E.M.M.D.L.N., P.N.V., T.S.F.S., E.M.V., A.G.M., N.F.C.R., J.T., K.R.C., E.N.H.C., A.M.M., J.C.M., F.R.C., T.R.F., A.C.Q., N.C.A., C.E.Z., T.J.K., B.S.M., B.H.M., R.V., B.M., R.L.A., C.B., D.D.D.A., J.E., P.P., H.C., M.B.D.M., M.F.S., An.A., J.L.C., W.F.L., S.G.L., L.M.R., J.S., T.R.S., G.B.M., E.D.S.F., M.A.L., J.L.L.M., H.E.M.N., H.L.D.Q., C.C.V., G.A.A.C., R.B., P.R.S., A.I.A., B.B.L.C., T.R.B., Y.O.F., H.F.M., J.F.D., C.A.P., M.R.S., L.V.F., J.R.L., J.A.C., J.J.D.T., G.D., N.D., F.C.D., R.G., A.L., A.V., F.C.V., A.I.A.I., L.A., F.D., V.H.G., E.M.J., D.N., M.C.P.M., J.C.N., F.C.D.S., K.J.F., R.G., T.H., J.E.H., M.P.P., J.J.P.I., M.R.P., D.D.J.R., J.B., E.B., I.B.D.S., M.J.F., J.F., P.V.F., M.C.G., C.L., J.C.L., B.E.V.Z., V.A.V., C.C., F.M.D., É.F., T.W.H., J.E.H., I.H., M.S., J.S., R.T., D.D., W.M., G.P.M., T.P., I.C.G.V., B.W.A., W.C., A.F., B.K., J.L.M.P., J.S.T., C.V., J.C., A.D.F., R.R.H., L.D.O.P., J.F.P., G.R., T.R.V.A., P.V.H., W.B., E.M.B., L.C.D.M.B., H.P.D.D., R.Z.G., T.G., G.P.G.G., B.H., A.B.J., Y.M., I.P.D.A.M., L.F.M.P., A.P., A.R., A.R.R., N.S., C.I.V., S.Z., E.L.Z., M.J.E., A.C., Y.A.C.M., D.F.C., J.B.P.C., B.M.F., D.G., M.H., M.K., G.L., L.T.M., M.T.N., A.A.O., M.M.P., H.R., M.R., V.V.S., M.N.U., G.V.D.H., E.V.T., T.M.V., M.A.A.R., C.B., H.B., S.C., L.F.C., W.F., C.F., R.L., C.M., I.M., G.A.P., A.T., L.E.U.G., D.V., R.Z., M.N.A., E.A.D.O., R.P.F., K.G.C., L.H., W.P.C., S.P., D.P., F.R.A., A.F.S., E.H.V.S., L.V.G., M.H., C.P. and Ht.S. provided data and had the opportunity to comment on the text; B.G.L., H.T., R.E., K.G.D., I.L.D.A., L.D.S.C., F.D.D.A.M., D.D.A.L.F., R.P.S., F.W., C.V.C., M.D.J.V.C., J.E.G., O.L.P., W.E.M., D.S., J.D.C.R., J.M., M.V.I., M.P.M., J.R.D.S.G., J.F.R., O.S.B., M.T.F.P., D.C.L., N.C.P., L.O.D., J.S., E.M.M.D.L.N., P.N.V., T.S.F.S., E.M.V., A.G.M., N.F.C.R., J.T., K.R.C., E.N.H.C., A.M.M., J.C.M., F.R.C., T.R.F., A.C.Q., N.C.A., C.E.Z., T.J.K., B.S.M., B.H.M., R.V., B.M., R.L.A., C.B., D.D.D.A., J.E., P.P., H.C., M.B.D.M., M.F.S., An.A., J.L.C., W.F.L., S.G.L., L.M.R., J.S., T.R.S., G.B.M., E.D.S.F., M.A.L., J.L.L.M., H.E.M.N., H.L.D.Q., C.C.V., G.A.A.C., R.B., P.R.S., A.I.A., B.B.L.C., T.R.B., Y.O.F., H.F.M., J.F.D., C.A.P., M.R.S., L.V.F., J.R.L., J.A.C., J.J.D.T., G.D., N.D., F.C.D., R.G., A.L., A.V., F.C.V., A.I.A.I., L.A., F.D., V.H.G., E.M.J., D.N., M.C.P.M., J.C.N., D.P.P.D.A., F.R.B., Y.K.B., R.D.S.C., F.A.C., F.C.D.S., K.J.F., R.G., T.H., J.E.H., M.P.P., J.J.P.I., M.R.P., D.D.J.R., J.B., E.B., I.B.D.S., M.J.F., J.F., P.V.F., M.C.G., C.L., J.C.L., B.E.V.Z., V.A.V., C.C., F.M.D., É.F., T.W.H., J.E.H., I.H., M.S., J.S., R.T., D.D., W.M., G.P.M., T.P., I.C.G.V., B.W.A., W.C., A.F., B.K., J.L.M.P., J.S.T., C.V., J.C., A.D.F., R.R.H., L.D.O.P., J.F.P., G.R., T.R.V.A., P.V.H., W.B., E.M.B., L.C.D.M.B., H.P.D.D., R.Z.G., T.G., G.P.G.G., B.H., A.B.J., Y.M., I.P.D.A.M., L.F.M.P., A.P., A.R., A.R.R., N.S., C.I.V., S.Z., E.L.Z., M.J.E., A.C., Y.A.C.M., D.F.C., J.B.P.C., B.M.F., D.G., M.H., M.K., G.L., L.T.M., M.T.N., A.A.O., M.M.P., H.R., M.R., V.V.S., M.N.U., G.V.D.H., E.V.T., T.M.V., M.A.A.R., C.B., H.B., S.C., L.F.C., W.F., C.F., R.L., C.M., I.M., G.A.P., A.T., L.E.U.G., D.V., R.Z., M.N.A., E.A.D.O., R.P.F., K.G.C., L.H., W.P.C., S.P., D.P., F.R.A., A.F.S., E.H.V.S., L.V.G., M.H., C.P. and Ht.S. approved the final version of the manuscript.

Competing interests

The authors declare no competing interests.

Additional information

Supplementary information The online version contains supplementary material available at <https://doi.org/10.1038/s42003-024-06937-5>.

Correspondence and requests for materials should be addressed to Hans ter Steege.

Peer review information *Communications Biology* thanks Sylvain Schmitt and the other, anonymous, reviewer(s) for their contribution to the peer review of this work. Primary Handling Editors: Luke Grinham and Kaliya Georgieva.

Reprints and permissions information is available at <http://www.nature.com/reprints>

Publisher's note Springer Nature remains neutral with regard to jurisdictional claims in published maps and institutional affiliations.

Open Access This article is licensed under a Creative Commons Attribution-NonCommercial-NoDerivatives 4.0 International License, which permits any non-commercial use, sharing, distribution and reproduction in any medium or format, as long as you give appropriate credit to the original author(s) and the source, provide a link to the Creative Commons licence, and indicate if you modified the licensed material. You do not have permission under this licence to share adapted material derived from this article or parts of it. The images or other third party material in this article are included in the article's Creative Commons licence, unless indicated otherwise in a credit line to the material. If material is not included in the article's Creative Commons licence and your intended use is not permitted by statutory regulation or exceeds the permitted use, you will need to obtain permission directly from the copyright holder. To view a copy of this licence, visit <http://creativecommons.org/licenses/by-nc-nd/4.0/>.

© The Author(s) 2024

Bruno Garcia Luize¹, Hanna Tuomisto^{2,3}, Robin Ekelschot⁴, Kyle G. Dexter^{5,6}, Iêda L. do Amaral⁷, Luiz de Souza Coelho⁷, Francisca Dionízia de Almeida Matos⁷, Diógenes de Andrade Lima Filho⁷, Rafael P. Salomão^{8,9}, Florian Wittmann^{10,11}, Carolina V. Castilho¹², Marcelo de Jesus Veiga Carim¹³, Juan Ernesto Guevara¹⁴, Oliver L. Phillips¹⁵, William E. Magnusson¹⁶, Daniel Sabatier¹⁷, Juan David Cardenas Revilla⁷, Jean-François Molino¹⁷, Mariana Victória Irueme⁷, Maria Pires Martins⁷, José Renan da Silva Guimarães¹⁸, José Ferreira Ramos⁷, Olaf S. Bánki⁴, Maria Teresa Fernandez Piedade¹¹, Dairon Cárdenas López^{19,149}, Nigel C. A. Pitman²⁰, Layon O. Demarchi¹¹, Jochen Schöngart¹¹, Evelyne Márcia Moraes de Leão Novo²¹, Percy Núñez Vargas²², Thiago Sanna Freire Silva²³, Eduardo Martins Venticinque²⁴, Angelo Gilberto Manzatto²⁵, Neidiane Farias Costa Reis²⁶, John Terborgh^{27,28}, Katia Regina Casula²⁶, Euridice N. Honorio Coronado^{29,30}, Abel Monteagudo Mendoza^{22,31}, Juan Carlos Montero^{7,32}, Flávia R. C. Costa¹⁶, Ted R. Feldpausch^{15,33}, Adriano Costa Quaresma¹¹, Nicolás Castaño Arboleda¹⁹, Charles Eugene Zartman⁷, Timothy J. Killeen³⁴, Beatriz S. Marimon³⁵, Ben Hur Marimon³⁵, Rodolfo Vasquez³¹, Bonifacio Mostacedo³⁶, Rafael L. Assis³⁷, Chris Baraloto³⁸, Dário Dantas do Amaral⁹, Julien Engel^{17,38}, Pascal Petronelli³⁹, Hernán Castellanos⁴⁰, Marcelo Brilhante de Medeiros⁴¹, Marcelo Fragomeni Simon⁴¹, Ana Andrade⁴², José Luís Camargo⁴², William F. Laurance²⁸, Susan G. W. Laurance²⁸, Lorena Maniguaje Rincón⁷, Juliana Schietti⁷, Thaiane R. Sousa⁴³, Gisele Biem Mori¹¹, Emanuelle de Sousa Farias⁴⁴, Maria Aparecida Lopes⁴⁵, José Leonardo Lima Magalhães^{46,47}, Henrique Eduardo Mendonça Nascimento⁷, Helder Lima de Queiroz⁴⁸, Caroline C. Vasconcelos⁴⁹, Gerardo A. Aymard C⁵⁰, Roel Brienen¹⁵, Pablo R. Stevenson⁵¹, Alejandro Araujo-Murakami⁵², Bruno Barçante Ladvoat Cintra⁵³, Tim R. Baker¹⁵, Yuri Oliveira Feitosa⁴⁹, Hugo F. Mogollón⁵⁴, Joost F. Duivenvoorden⁵⁵, Carlos A. Peres⁵⁶, Miles R. Silman⁵⁷, Leandro Valle Ferreira⁹, José Rafael Lozada⁵⁸, James A. Comiskey^{59,60}, José Julio de Toledo⁶¹, Gabriel Damasco⁶², Nállarett Dávila^{1,150}, Freddie C. Draper⁶³, Roosevelt García-Villacorta^{64,65}, Aline Lopes⁶⁶, Alberto Vicentini¹⁶, Fernando Cornejo Valverde⁶⁷, Alfonso Alonso⁶⁰, Luzmila Arroyo⁵², Francisco Dallmeier⁶⁰, Vitor H. F. Gomes^{68,69}, Eliana M. Jimenez⁷⁰, David Neill⁷¹, Maria Cristina Peñuela Mora⁷², Janaina Costa Noronha⁷³, Daniel P. P. de Aguiar^{74,75}, Flávia Rodrigues Barbosa⁷³, Yennie K. Bredin⁷⁶, Rainiellen de Sá Carpanedo⁷³, Fernanda Antunes Carvalho^{16,77}, Fernanda Coelho de Souza^{15,16}, Kenneth J. Feeley^{78,79}, Rogerio Gribel⁷, Torbjørn Haugaasen⁷⁶, Joseph E. Hawes⁷⁶, Marcelo Petratti Pansonato^{7,80}, John J. Pipoly III⁸¹, Marcos Ríos Paredes⁸², Domingos de Jesus Rodrigues⁷³, Jos Barlow⁸³, Erika Berenguer^{83,84}, Izaias Brasil da Silva⁸⁵, Maria Julia Ferreira⁸⁶, Joice Ferreira⁴⁷, Paul V. A. Fine⁸⁷, Marcelino Carneiro Guedes⁸⁸, Carolina Levis⁸⁹, Juan Carlos Licona³², Boris Eduardo Villa Zegarra⁹⁰, Vincent Antoine Vos⁹¹, Carlos Cerón⁹², Flávia Machado Durgante^{10,11}, Émile Fonty^{17,93}, Terry W. Henkel⁹⁴, John Ethan Householder¹⁰, Isau Huamantupa-Chuquimaco⁹⁵, Marcos Silveira⁹⁶, Juliana Stropp⁹⁷, Raquel Thomas⁹⁸, Doug Daly⁹⁹, William Milliken¹⁰⁰, Guido Pardo Molina⁹¹, Toby Pennington^{6,33}, Ima Célia Guimarães Vieira⁹, Bianca Weiss Albuquerque¹¹, Wegliane Campelo⁶¹, Alfredo Fuentes^{101,102}, Bente Klitgaard¹⁰³, José Luis Marcelo Pena¹⁰⁴, J. Sebastián Tello¹⁰¹, Corine Vriesendorp²⁰, Jerome Chave¹⁰⁵, Anthony Di Fiore^{106,107}, Renato Richard Hilário⁶¹, Luciana de Oliveira Pereira³³, Juan Fernando Phillips¹⁰⁸, Gonzalo Rivas-Torres^{107,109}, Tinde R. van Andel^{4,110}, Patricio von Hildebrand¹¹¹, William Balee¹¹², Edelcilio Marques Barbosa⁷, Luiz Carlos de Matos Bonates⁷, Hilda Paulette Dávila Doza⁸², Ricardo Zárate Gómez¹¹³, Therany Gonzales¹¹⁴, George Pepe Gallardo Gonzales⁸², Bruce Hoffman¹¹⁵, André Braga Junqueira¹¹⁶, Yadvinder Malhi⁸⁴, Ires Paula de Andrade Miranda⁷, Linder Felipe Mozombite Pinto⁸², Adriana Prieto¹¹⁷, Agustín Rudas¹¹⁷, Ademir R. Ruschel⁴⁷,

Natalino Silva¹¹⁸, César I. A. Vela¹¹⁹, Stanford Zent¹²⁰, Egleé L. Zent¹²⁰, María José Endara¹²⁴, Angela Cano^{51,121}, Yrma Andreina Carrero Márquez¹²², Diego F. Correa^{51,123}, Janaina Barbosa Pedrosa Costa⁸⁸, Bernardo Monteiro Flores⁸⁹, David Galbraith¹⁵, Milena Holmgren¹²⁴, Michelle Kalamandeen¹²⁵, Guilherme Lobo¹²⁶, Luis Torres Montenegro¹²⁷, Marcelo Trindade Nascimento¹²⁸, Alexandre A. Oliveira⁸⁰, Maihyra Marina Pombo⁷, Hirma Ramirez-Angulo¹²⁹, Maira Rocha¹¹, Veridiana Vizoni Scudeller¹³⁰, Maria Natalia Umaña¹³¹, Geertje van der Heijden¹³², Emilio Vilanova Torre^{129,133}, Tony Mori Vargas¹³⁴, Manuel Augusto Ahuite Reategui¹³⁵, Cláudia Baider^{80,136}, Henrik Balslev¹³⁷, Sasha Cárdenas⁵¹, Luisa Fernanda Casas⁵¹, William Farfan-Rios^{22,57}, Cid Ferreira^{7,151}, Reynaldo Linares-Palomino¹³⁸, Casimiro Mendoza^{138,139}, Italo Mesones⁸⁷, Germaine Alexander Parada⁵², Armando Torres-Lezama¹²⁹, Ligia Estela Urrego Giraldo¹⁴⁰, Daniel Villarroel^{52,141}, Roderick Zagt¹⁴², Miguel N. Alexiades¹⁴³, Edmar Almeida de Oliveira¹³⁵, Riley P. Fortier¹⁴⁴, Karina Garcia-Cabrera⁵⁷, Lionel Hernandez⁴⁰, Walter Palacios Cuenca¹⁴⁴, Susamar Pansini²⁶, Daniela Pauletto¹⁴⁵, Freddy Ramirez Arevalo¹³⁴, Adeilza Felipe Sampaio²⁶, Elvis H. Valderrama Sandoval^{134,146}, Luis Valenzuela Gamarra³¹, Marina Hirota¹⁴⁷, Clarisse Palma-Silva¹ & Hans ter Steege^{4,148} ✉

¹Departamento de Biologia Vegetal, Instituto de Biologia, Universidade Estadual de Campinas – UNICAMP, Campinas, SP, Brazil. ²Section of Ecoinformatics and Biodiversity, Department of Biology, Aarhus University, Aarhus, Denmark. ³Department of Biology, University of Turku, Turku, Finland. ⁴Naturalis Biodiversity Center, Leiden, The Netherlands. ⁵Department of Life Sciences and Systems Biology, University of Turin, Turin, Italy. ⁶Tropical Diversity Section, Royal Botanic Garden Edinburgh, Edinburgh, Scotland, UK. ⁷Coordenação de Biodiversidade, Instituto Nacional de Pesquisas da Amazônia - INPA, Manaus, AM, Brazil. ⁸Programa Professor Visitante Nacional Sênior na Amazônia - CAPES, Universidade Federal Rural da Amazônia, Belém, PA, Brazil. ⁹Coordenação de Botânica, Museu Paraense Emílio Goeldi, Belém, PA, Brazil. ¹⁰Wetland Department, Institute of Geography and Geoecology, Karlsruhe Institute of Technology - KIT, Rastatt, Germany. ¹¹Ecology, Monitoring and Sustainable Use of Wetlands (MAUA), Instituto Nacional de Pesquisas da Amazônia - INPA, Petrópolis, Manaus, AM, Brazil. ¹²Centro de Pesquisa Agroflorestal de Roraima, Embrapa Roraima, Boa Vista, RR, Brazil. ¹³Departamento de Botânica, Instituto de Pesquisas Científicas e Tecnológicas do Amapá - IEPA, Rodovia JK, Macapá, AP, Brazil. ¹⁴Grupo de Investigación en Ecología y Evolución en los Trópicos-EETrop, Universidad de las Américas, Quito, Ecuador. ¹⁵School of Geography, University of Leeds, Woodhouse Lane, Leeds, UK. ¹⁶Coordenação de Pesquisas em Ecologia, Instituto Nacional de Pesquisas da Amazônia - INPA, Manaus, AM, Brazil. ¹⁷AMAP (botAnique et Modélisation de l'Architecture des Plantes et des végétations), Université de Montpellier, CIRAD, CNRS, INRAE, IRD, Montpellier, France. ¹⁸Amcel Amapá Florestal e Celulose S.A, Rua Claudio Lucio - S/N, Novo Horizonte, Santana, AP, Brazil. ¹⁹Herbario Amazónico Colombiano, Instituto SINCHI, Bogotá, Colombia. ²⁰Science and Education, The Field Museum, Chicago, IL, USA. ²¹Divisão de Sensoriamento Remoto – DSR, Instituto Nacional de Pesquisas Espaciais – INPE, São José dos Campos, SP, Brazil. ²²Herbario Vargas, Universidad Nacional de San Antonio Abad del Cusco, Cusco, Cuzco, Peru. ²³Biological and Environmental Sciences, University of Stirling, Stirling, UK. ²⁴Centro de Biociências, Departamento de Ecologia, Universidade Federal do Rio Grande do Norte, Natal, RN, Brazil. ²⁵Departamento de Biologia, Universidade Federal de Rondônia, Porto Velho, RO, Brazil. ²⁶Programa de Pós- Graduação em Biodiversidade e Biotecnologia PPG- Bionorte, Universidade Federal de Rondônia, Porto Velho, RO, Brazil. ²⁷Department of Biology and Florida Museum of Natural History, University of Florida, Gainesville, FL, USA. ²⁸Centre for Tropical Environmental and Sustainability Science and College of Science and Engineering, James Cook University, Cairns, QLD, Australia. ²⁹Instituto de Investigaciones de la Amazonía Peruana (IIAP), Iquitos, Loreto, Peru. ³⁰School of Geography and Sustainable Development, University of St Andrews, Irvine Building, St Andrews, UK. ³¹Jardín Botánico de Missouri, Oxapampa, Pasco, Peru. ³²Instituto Boliviano de Investigación Forestal, Santa Cruz, Bolivia. ³³Geography, College of Life and Environmental Sciences, University of Exeter, Rennes Drive, Exeter, UK. ³⁴Agteca-Amazonica, Santa Cruz, Bolivia. ³⁵Programa de Pós- Graduação em Ecologia e Conservação, Universidade do Estado de Mato Grosso, Nova Xavantina, MT, Brazil. ³⁶Facultad de Ciencias Agrícolas, Universidad Autónoma Gabriel René Moreno, Santa Cruz, Santa Cruz, Bolivia. ³⁷Biodiversity and Ecosystem Services, Instituto Tecnológico Vale, Belém, Pará, Brazil. ³⁸International Center for Tropical Botany (ICTB) Department of Biological Sciences, Florida International University, Miami, FL, USA. ³⁹Cirad UMR Ecofog, AgrosParisTech, CNRS, INRAE, Univ Guyane, Campus agronomique, Kourou Cedex, France. ⁴⁰Centro de Investigaciones Ecológicas de Guayana, Universidad Nacional Experimental de Guayana, Calle Chile, urbaniz Chilemex, Puerto Ordaz, Bolívar, Venezuela. ⁴¹Embrapa Recursos Genéticos e Biotecnologia, Parque Estação Biológica, Prédio da Botânica e Ecologia, Brasília, DF, Brazil. ⁴²Projeto Dinâmica Biológica de Fragmentos Florestais, Instituto Nacional de Pesquisas da Amazônia - INPA, Petrópolis, Manaus, AM, Brazil. ⁴³Programa de Pós-Graduação em Ecologia, Instituto Nacional de Pesquisas da Amazônia - INPA, Petrópolis, Manaus, AM, Brazil. ⁴⁴Laboratório de Ecologia de Doenças Transmissíveis da Amazônia (EDTA), Instituto Leônidas e Maria Deane, Manaus, AM, Brazil. ⁴⁵Instituto de Ciências Biológicas, Universidade Federal do Pará, Belém, PA, Brazil. ⁴⁶Programa de Pós-Graduação em Ecologia, Universidade Federal do Pará, Belém, PA, Brazil. ⁴⁷Empresa Brasileira de Pesquisa Agropecuária, Embrapa Amazônia Oriental, Trav. Dr. Enéas Pinheiro s/n°, Belém, PA, Brazil. ⁴⁸Diretoria Técnico-Científica, Instituto de Desenvolvimento Sustentável Mamirauá, Tefé, AM, Brazil. ⁴⁹Programa de Pós-Graduação em Biologia (Botânica), Instituto Nacional de Pesquisas da Amazônia - INPA, Av. André Araújo, 2936, Petrópolis, Manaus, AM, Brazil. ⁵⁰Programa de Ciencias del Agro y el Mar, Herbario Universitario (PORT), UNELLEZ-Guanare, Guanare, Portuguesa, Venezuela. ⁵¹Laboratório de Ecologia de Bosques Tropicales y Primatología, Universidad de los Andes, Bogotá, DC, Colombia. ⁵²Museo de Historia Natural Noel Kempff Mercado, Universidad Autónoma Gabriel Rene Moreno, Santa Cruz, Santa Cruz, Bolivia. ⁵³School of Geography, Earth and Environmental Sciences & Birmingham Institute for Forest Research, University of Birmingham, Edgbaston, Birmingham, UK. ⁵⁴Endangered Species Coalition, Silver Spring, MD, USA. ⁵⁵Institute of Biodiversity and Ecosystem Dynamics, University of Amsterdam, Amsterdam, The Netherlands. ⁵⁶School of Environmental Sciences, University of East Anglia, Norwich, UK. ⁵⁷Biology Department and Center for Energy, Environment and Sustainability, Wake Forest University, Winston Salem, NC, USA. ⁵⁸Facultad de Ciencias Forestales y Ambientales, Instituto de Investigaciones para el Desarrollo Forestal, Universidad de los Andes, Via Chorro de Milla, 5101, Mérida, Mérida, Venezuela. ⁵⁹Inventory and Monitoring Program, National Park Service, Fredericksburg, VA, USA. ⁶⁰Center for Conservation and Sustainability, Smithsonian Conservation Biology Institute, Washington, DC, USA. ⁶¹Universidade Federal do Amapá, Ciências Ambientais, Macapá, AP, Brazil. ⁶²Gothenburg Global Biodiversity Centre, University of Gothenburg, Gothenburg, Sweden. ⁶³Department of Geography and Planning, University of Liverpool, Liverpool, UK. ⁶⁴Centro para la Restauración y Bioeconomía Sostenible - CREBIOS, Lima 15088, Peru. ⁶⁵Peruvian Center for Biodiversity and Conservation (PCBC), Iquitos, Loreto, Peru. ⁶⁶Postgraduate Program in Clean Technologies, UniCesumar and Cesumar Institute of Science, Technology, and Innovation (ICETI), UniCesumar, Maringá, PR, Brazil. ⁶⁷Andes to Amazon Biodiversity Program, Madre de Dios, Madre de Dios, Peru. ⁶⁸Escola de Negócios Tecnologia e Inovação, Centro Universitário do Pará, Belém, PA, Brazil. ⁶⁹Environmental Science Program, Geosciences Department, Universidade Federal do Pará, Belém, PA, Brazil. ⁷⁰Grupo de Ecología y Conservación de Fauna y Flora Silvestre, Instituto Amazónico de Investigaciones Imani, Universidad Nacional de Colombia sede Amazonia, Leticia, Amazonas, Colombia. ⁷¹Universidad Estatal Amazónica, Puyo, Pastaza, Ecuador. ⁷²Universidad Regional Amazónica IKIAM, Tena, Napo, Ecuador. ⁷³ICNHS, Federal University of Mato Grosso, Sinop, MT, Brazil. ⁷⁴Procuradoria-Geral de Justiça, Ministério Público do Estado do Amazonas, Manaus, AM, Brazil. ⁷⁵Coordenação de Dinâmica Ambiental, Instituto Nacional de Pesquisas da Amazônia - INPA, Petrópolis, Manaus, AM, Brazil. ⁷⁶Norwegian University of Life

Sciences (NMBU), Faculty of Environmental Sciences and Natural Resource Management, Aas, Norway. ⁷⁷Universidade Federal de Minas Gerais, Instituto de Ciências Biológicas, Departamento de Genética, Ecologia e Evolução, Belo Horizonte, MG, Brazil. ⁷⁸Department of Biology, University of Miami, Coral Gables, FL, USA. ⁷⁹Fairchild Tropical Botanic Garden, Coral Gables, FL, USA. ⁸⁰Instituto de Biociências - Dept. Ecologia, Universidade de Sao Paulo - USP, Rua do Matão, Trav. 14, no. 321, Cidade Universitária, São Paulo, SP, Brazil. ⁸¹Dept. Biological Sciences, Broward County Parks and Recreation, Boca Raton, Oakland Park, FL, USA. ⁸²Servicios de Biodiversidad EIRL, Iquitos, Loreto, Peru. ⁸³Lancaster Environment Centre, Lancaster University, Lancaster, Lancashire, UK. ⁸⁴Environmental Change Institute, School of Geography and the Environment, University of Oxford, Oxford, UK. ⁸⁵Postgraduate program in Biodiversity and Biotechnology – Bionorte, Federal University of Acre, Rio Branco, AC, Brazil. ⁸⁶Scientific research program, Juruá Institute, Aleixo, Manaus, AM, Brazil. ⁸⁷Department of Integrative Biology, University of California, Berkeley, CA, USA. ⁸⁸Empresa Brasileira de Pesquisa Agropecuária, Embrapa Amapá, Macapá, AP, Brazil. ⁸⁹Graduate Program in Ecology, Federal University of Santa Catarina (UFSC), Campus Universitário - Córrego Grande, Florianópolis, SC, Brazil. ⁹⁰Dirección de Evaluación Forestal y de Fauna Silvestre, Magdalena del Mar, Peru. ⁹¹Instituto de Investigaciones Forestales de la Amazonia, Universidad Autónoma del Beni José Ballivián, Campus Universitario Final, Riberalta, Beni, Bolivia. ⁹²Escuela de Biología Herbario Alfredo Paredes, Universidad Central, Quito, Pichincha, Ecuador. ⁹³Direction régionale de la Guyane, Office national des forêts, Cayenne, French Guiana. ⁹⁴Department of Biological Sciences, California State Polytechnic University, Arcata, CA, USA. ⁹⁵Herbario HAG, Universidad Nacional Amazónica de Madre de Dios (UNAMAD), Puerto Maldonado, Madre de Dios, Peru. ⁹⁶Centro de Ciências Biológicas e da Natureza, Universidade Federal do Acre, Rio Branco, AC, Brazil. ⁹⁷Museo Nacional de Ciencias Naturales (MNCN-CSIC), Madrid, Spain. ⁹⁸Iwokrama International Centre for Rain Forest Conservation and Development, Georgetown, Guyana. ⁹⁹New York Botanical Garden, Bronx, New York, NY, USA. ¹⁰⁰Department for Ecosystem Stewardship, Royal Botanic Gardens, Kew, Richmond, Surrey, UK. ¹⁰¹Latin America Department, Missouri Botanical Garden, St. Louis, MO, USA. ¹⁰²Herbario Nacional de Bolivia, Instituto de Ecología, Universidad Mayor de San Andres, Carrera de Biología, La Paz, Bolivia. ¹⁰³Department for Accelerated Taxonomy, Royal Botanic Gardens, Kew, Richmond, Surrey, UK. ¹⁰⁴Laboratorio de Plantas Vasculares y Herbario ISV, Universidad Nacional de Jaén, Carretera Jaén San Ignacio Km 23, Jaén, Cajamarca, Peru. ¹⁰⁵Laboratoire Evolution et Diversité Biologique, CNRS and Université Paul Sabatier, Toulouse, France. ¹⁰⁶Department of Anthropology, University of Texas at Austin, Austin, TX, USA. ¹⁰⁷Estación de Biodiversidad Tiputini, Colegio de Ciencias Biológicas y Ambientales, Universidad San Francisco de Quito-USFQ, Quito, Pichincha, Ecuador. ¹⁰⁸Fundación Puerto Rastrojo, Bogotá, DC, Colombia. ¹⁰⁹Department of Wildlife Ecology and Conservation, University of Florida, Gainesville, FL, USA. ¹¹⁰Biosystematics group, Wageningen University, Wageningen, The Netherlands. ¹¹¹Fundación Estación de Biología, Bogotá, DC, Colombia. ¹¹²Department of Anthropology, Tulane University, New Orleans, LA, USA. ¹¹³PROTERRA, Instituto de Investigaciones de la Amazonía Peruana (IIAP), Iquitos, Loreto, Peru. ¹¹⁴ACEER Foundation, Puerto Maldonado, Madre de Dios, Peru. ¹¹⁵Amazon Conservation Team, Arlington, VA, USA. ¹¹⁶Institut de Ciència i Tecnologia Ambientals, Universitat Autònoma de Barcelona, Barcelona, Spain. ¹¹⁷Instituto de Ciencias Naturales, Universidad Nacional de Colombia, Bogotá, DC, Colombia. ¹¹⁸Instituto de Ciência Agrárias, Universidade Federal Rural da Amazônia, Belém, PA, Brazil. ¹¹⁹Escuela Profesional de Ingeniería Forestal, Universidad Nacional de San Antonio Abad del Cusco, Puerto Maldonado, Madre de Dios, Peru. ¹²⁰Laboratory of Human Ecology, Instituto Venezolano de Investigaciones Científicas - IVIC, Caracas, DC, Venezuela. ¹²¹Cambridge University Botanic Garden, Cambridge University, 1 Brookside, Cambridge, UK. ¹²²Programa de Maestria de Manejo de Bosques, Universidad de los Andes, Mérida, Mérida, Venezuela. ¹²³Centre for Biodiversity and Conservation Science CBCS, The University of Queensland, Brisbane, QLD, Australia. ¹²⁴Resource Ecology Group, Wageningen University & Research, Lumen, Wageningen, Gelderland, The Netherlands. ¹²⁵Unique land use GmbH, Freiburg im Breisgau, Germany. ¹²⁶Núcleo de Estudos e Pesquisas Ambientais, Universidade Estadual de Campinas – UNICAMP, Campinas, SP, Brazil. ¹²⁷Herbarium Amazonense (AMAZ), Universidad Nacional de la Amazonia Peruana, Iquitos, Loreto, Peru. ¹²⁸Laboratório de Ciências Ambientais, Universidade Estadual do Norte Fluminense, Campos dos Goytacazes, RJ, Brazil. ¹²⁹Instituto de Investigaciones para el Desarrollo Forestal (INDEFOR), Universidad de los Andes, Conjunto Forestal, Mérida, Mérida, Venezuela. ¹³⁰Departamento de Biología, Universidade Federal do Amazonas - UFAM – Instituto de Ciências Biológicas – ICB1, Manaus, AM, Brazil. ¹³¹Department of Ecology and Evolutionary Biology, University of Michigan, Ann Arbor, MI, USA. ¹³²Faculty of Social Sciences, University of Nottingham, University Park, Nottingham, UK. ¹³³Wildlife Conservation Society (WCS), 2300 Southern Boulevard, Bronx, New York, NY, USA. ¹³⁴Facultad de Biología, Universidad Nacional de la Amazonia Peruana, Iquitos, Loreto, Peru. ¹³⁵Medio Ambiente, PLUSPRETOL, Iquitos, Loreto, Peru. ¹³⁶The Mauritius Herbarium, Agricultural Services, Ministry of Agro-Industry and Food Security, Reduit, Mauritius. ¹³⁷Department of Biology, Aarhus University, Aarhus C, Aarhus, Denmark. ¹³⁸Escuela de Ciencias Forestales (ESFOR), Universidad Mayor de San Simon (UMSS), Sacta, Cochabamba, Bolivia. ¹³⁹FOMABO, Manejo Forestal en las Tierras Tropicales de Bolivia, Sacta, Cochabamba, Bolivia. ¹⁴⁰Departamento de Ciencias Forestales, Universidad Nacional de Colombia, Medellín, Antioquia, Colombia. ¹⁴¹Fundación Amigos de la Naturaleza (FAN), Santa Cruz, Bolivia. ¹⁴²Tropenbos International, Ede, The Netherlands. ¹⁴³School of Anthropology and Conservation, University of Kent, Marlowe Building, Canterbury, Kent, UK. ¹⁴⁴Herbario Nacional del Ecuador, Universidad Técnica del Norte, Quito, Pichincha, Ecuador. ¹⁴⁵Instituto de Biodiversidade e Florestas, Universidade Federal do Oeste do Pará, Rua Vera Paz, Campus Tapajós, Santarém, PA, Brazil. ¹⁴⁶Department of Biology, University of Missouri, St. Louis, MO, USA. ¹⁴⁷Department of Physics, Federal University of Santa Catarina, Florianópolis, SC, Brazil. ¹⁴⁸Quantitative Biodiversity Dynamics, Utrecht University, Padualaan 8, Utrecht, The Netherlands. ¹⁴⁹Deceased: Dairon Cárdenas López. ¹⁵⁰Deceased: Nállarett Dávila. ¹⁵¹Deceased: Cid Ferreira. ✉ e-mail: hans.tersteeg@naturalis.nl